

1 **Chemical and U-Sr isotopic variations in stream and source waters of the Strengbach**
2 **watershed (Vosges mountains; France)**

3 ¹Pierret M.C., ¹Stille P., ¹⁻²Prunier J., ¹Viville D. and ¹Chabaux F.

4

5 (1) Laboratoire d'Hydrologie et de Géochimie de Strasbourg, EOSt, Université de
6 Strasbourg/CNRS, 1 rue Blessig 67084 Strasbourg, France.

7 (2) Present address LMTG – Université Paul Sabatier, CNRS/IRD, Observatoire Midi-
8 Pyrénées, 14, avenue Edouard Belin, 31400 Toulouse, France.

9

10 Correspondence to: Marie Claire Pierret marie-claire.pierret@unistra.fr

11

12 **Abstract**

13 This is the first comprehensive study dealing with major and trace element data as well as ⁸⁷Sr/⁸⁶Sr
14 isotope and (²³⁴U/²³⁸U) activity ratios (AR) determined on the totality of springs and brooks of the
15 Strengbach catchment. It shows that the small and more or less monolithic catchment drains
16 different sources and streamlets with very different isotopic and geochemical signatures. Different
17 parameters control the diversity of the source characteristics. Of importance is especially the
18 hydrothermal overprint of the granitic bedrock, which was stronger for the granite from the northern
19 slope; also significant are the different meteoric alteration processes of the bedrock causing the
20 formation of 0.5 to 9 meter thick saprolite and above the formation of an up to 1m thick soil system.
21 These processes mainly account for springs and brooks from the northern slope having higher
22 Ca/Na, Mg/Na, Sr/Na ratios but lower ⁸⁷Sr/⁸⁶Sr isotopic ratios than those from the southern slope.
23 The chemical compositions of the source waters in the Strengbach catchment are only to a small
24 extent the result of alteration of primary bedrock minerals and rather reflect
25 dissolution/precipitation processes of secondary mineral phases like clay minerals.

26 The ($^{234}\text{U}/^{238}\text{U}$) AR, however, are decoupled from the $^{87}\text{Sr}/^{86}\text{Sr}$ isotope system and reflect to some
27 extent the level of altitude of the source and, thus, the degree of alteration of the bedrock. The
28 sources emerging at high altitudes have circulated through already weathered materials (saprolite
29 and fractured bedrock depleted in ^{234}U) implying ($^{234}\text{U}/^{238}\text{U}$) AR <1, which is uncommon for surface
30 waters. Preferential flow paths along constant fractures in the bedrocks might explain the over time
31 homogeneous U AR of the different spring waters. However, the geochemical and isotopic
32 variations of stream waters at the outlet of the catchment are controlled by variable contributions of
33 different springs depending on the hydrological conditions.

34 It appears that the ($^{234}\text{U}/^{238}\text{U}$) AR is an appropriate very important tracer for studying and
35 deciphering the contribution of the different source fluxes at the catchment scale because this
36 unique geochemical parameter is different for each individual spring and at the same time remains
37 unchanged for each of the springs with changing discharge and fluctuating hydrological conditions.
38 This study further highlights the important impact of different and independent water pathways in
39 fractured granite controlling the different geochemical and isotopic signatures of the waters. Despite
40 the fact that soils and vegetation cover have a great influence on the water cycle balance
41 (evapotranspiration, drainage, runoff), the chemical compositions of waters are strongly modified
42 by processes occurring in deep saprolite and bedrock rather than in soils along the specific water
43 pathways.

44

45 Keywords: U activity ratios, Sr isotopes, spring and stream water chemistry, weathering,
46 Strengbach catchment.

47

48 **1. Introduction**

49 Large rivers carry erosion products from the different drainage areas and, therefore, are pathways of
50 continental weathering products that finally enter the oceans. Thus, they fetch the various chemical
51 and isotopical characteristics of the different drainage basins and, therefore, allow to elucidate

52 erosion processes, derive erosion rates and to illustrate biogeochemical cycling of elements. Many
53 of the major world rivers are well documented with major and trace element and isotope data on
54 dissolved and suspended phases, which provide the different factors controlling chemical and
55 physical denudation (Degens et al., 1991; Dupré et al., 2003; Gaillardet et al., 1999; Martin and
56 Meybeck, 1979 ; Négrel et al., 1993). At the large catchment scale, the stream waters chemical
57 composition is generally the result of mixing between phases derived from the different main
58 lithologies (e.g., Bickle et al., 2006; Blum et al., 1998; Chabaux et al., 2001; Millot et al., 2003;
59 Steinmann and Stille, 2009; Tipper et al., 2006; Zakharova et al., 2007). The impact and the role of
60 vegetation cover and soils on the chemical or isotopical evolution of erosion signals in waters of
61 small catchments have very recently been discussed (Laudon et al., 2004; Cenko-Tok et al., 2009;
62 Cividini et al., 2011; Engstrom et al., 2010; Kohler et al., 2014; Lemarchand et al., 2010; Zakharova
63 et al., 2007). Determination of parameters controlling the chemical composition of superficial
64 waters is important for a correct modeling of the future evolution of ecosystems in response to
65 external natural or anthropogenic forcing such as climate evolution and atmospheric pollution (trace
66 metal depositions, acid rain etc.). Among these parameters water/rock interactions (including
67 secondary phases such as clays), hydrological processes and biological activities play an important
68 role in affecting mobilization, (re)cycling and fractionation of elements; their specific influences on
69 weathering processes at the watershed scale remains a matter of discussion (Brantley et al., 2008).
70 Because natural systems are subject to complex and multiple reactions, the combination of different
71 geochemical and isotopical tools is necessary to decipher the different natural processes. $^{87}\text{Sr}/^{86}\text{Sr}$
72 isotopic ratios and ($^{234}\text{U}/^{238}\text{U}$) AR have successfully been used in the discussion of hydrological and
73 hydrochemical processes at the catchment scale (e.g. Riotte and Chabaux, 1999; Tricca et al., 1999;
74 Aubert et al., 2002; Bagard et al., 2011; Bickle et al., 2005; Bonotto and Andrews, 2000; Chabaux
75 et al., 2011; Durand et al., 2005; Schaffhauser et al., 2014). Indeed, when the U system has been
76 closed for approximately 1 million years, minerals and rocks are in secular equilibrium and
77 activities of all parents and daughters from ^{238}U decay chain are identical and the ($^{234}\text{U}/^{238}\text{U}$) AR is

78 equal to 1. However, this ratio can fractionate during chemical weathering when ^{234}U is more easily
79 released into solution by the combined effects of 1) direct recoil of ^{234}Th near grain boundaries out
80 of mineral and 2) preferential release from crystal lattices that are damaged by energetic α -decay
81 (e.g. Bourdon et al., 2009; Chabaux et al., 2003; 2008; DePaolo et al., 2006; 2012; Osmond and
82 Ivanovich, 1992 and references therein). Therefore, natural waters (stream, spring, groundwaters,
83 seawaters) are generally in excess of ^{234}U with $(^{234}\text{U}/^{238}\text{U})$ AR >1 (Andrews and Kay, 1983;
84 Camacho et al., 2010; Chabaux et al., 2003, 2008; Dosseto et al., 2008, 2012; Gryzmko et al., 2007;
85 Osmond and Ivanovich, 1992; Paces et al., 2002; Pierret et al., 2012; Vigier et al., 2001, 2006).
86 Consequently, $(^{234}\text{U}/^{238}\text{U})$ AR in superficial waters allow to identify river- flow patterns, and
87 hydrological mixing by tracing the sources of water and recording mixing between superficial and
88 groundwaters characterized by different U AR. Thus the $(^{234}\text{U}/^{238}\text{U})$ AR change along river flows
89 and in function of hydrological mixing (e.g., Chabaux et al., 2001; Durand et al., 2005; Maher et al.,
90 2006; Osmond and 1982; Paces et al., 2002; Riotte et Chabaux, 1999).

91 In the present paper we focus on a small, more or less monolithic drainage basin, the experimental
92 Strengbach catchment (Vosges mountains, NE France). Several studies have shown that the
93 vegetation cover, the atmospheric deposition, the secondary minerals and the biological recycling
94 play an important role in controlling the geochemical signatures of soil solutions (Brioshi et al.,
95 2012; Lemarchand et al., 2010; Lemarchand et al., 2012; Prunier, 2008; Stille et al., 2006, 2009,
96 2011, 2012). The impact of physico-chemical processes in soil on the chemical balance of waters at
97 the outlet is rather weak. For instance, the mean annual flux of Ca in soil solution at 60 cm depth
98 represents 5 to 20% of the annual flux at the outlet, depending on the type of vegetation or soil
99 (Cenki-Tok et al., 2009). Therefore, the chemical compositions of waters are mainly controlled by
100 interactions occurring with the deep saprolite and bedrock rather than with soils.

101 A previous U isotope study performed on waters from the Strengbach streamlet shows a decrease of
102 the $(^{234}\text{U}/^{238}\text{U})$ AR from 1.02 to 0.96 when the discharge of the stream increases (Riotte and
103 Chabaux, 1999). Such an isotopic evolution has been interpreted as mixing between a water body

104 enriched in ^{234}U , which is supposed to have interacted with a granitic bed rock at secular
105 equilibrium, and waters with a ($^{234}\text{U}/^{238}\text{U}$) AR below unity pointing to mobilization of U from
106 material that has already been weathered. Similarly, the streamlets $^{87}\text{Sr}/^{86}\text{Sr}$ isotope ratios collected
107 during low flow periods have low $^{87}\text{Sr}/^{86}\text{Sr}$ ratios than during high water flow events (Aubert et al.,
108 2002). The Sr signature at low discharge has been explained by important contributions of waters
109 from the deep soil profile during the recession stage, whereas higher $^{87}\text{Sr}/^{86}\text{Sr}$ isotope ratios at
110 higher discharge are due to important contributions of waters from the saturated area of the
111 catchment.

112 In order to define more precisely temporal and spatial variations of the hydrochemistry of the
113 streamlet and the different springs and to evaluate the major and trace element sources and the
114 processes controlling this element supply to the freshwaters, additional ($^{234}\text{U}/^{238}\text{U}$) AR, $^{87}\text{Sr}/^{86}\text{Sr}$
115 isotopic ratios and major and trace element concentrations were analyzed in the different source
116 waters collected during two different hydrological seasons (2004-2006) and compared to those of
117 the streamlet.

118

119 **2. Site description**

120 The Strengbach catchment is a small granitic watershed (0.8 km²) where meteorological,
121 hydrological and geochemical data are recorded since 1986 (Observatoire Hydro-Géochimique de
122 l'Environnement; OHGE; <http://ohge.u-strasbg.fr>). The first studies were performed in order to
123 understand the impact of acid rain on the forested ecosystem (Dambrine et al. 1991, 1992a,b; Probst
124 et al. 1990, 1992a, b). The catchment is situated in the Vosges Mountains (NE France) at altitudes
125 between 880 and 1150 m (amsl) and has strongly inclined slopes (mean 15°; Fig. 1).

126 The climate is temperate oceanic mountainous (mean annual temperature of 6°C; mean monthly
127 temperature range from -2 to 14°C) with an average rainfall of 1400 mm/yr (ranging between 890
128 and 1630 mm/yr over the period 1986-2006) and with snowfall during 2-4 month/yr (Probst and
129 Viville, 1997; Viville et al., 2012; OHGE Data). The mean annual runoff for the same period is of

130 853 mm ($26.9 \text{ L s}^{-1} \text{ km}^{-2}$) and ranges from 525 to 1147 mm over 1986-2006 (Ladouche et al., 2001;
131 Probst and Vivile, 1997; OHGE data). The evapotranspiration (ETP) has been evaluated to be about
132 40% on the site (Aubert, 2001; Probst et al., 1992).

133 The bedrock is mainly composed of a Hercynian base-poor granite ($332 \pm 2 \text{ Ma}$) (Boutin et al.,
134 1995), with low Ca and Mg contents (less than 1% for both); it suffered different degrees of
135 hydrothermal alteration some 180 Ma ago (Fichter et al., 1998). In addition to the granite, which is
136 strongly hydrothermally altered on the northern slope and comparatively weakly altered on the
137 southern slope, small microgranite and gneiss bodies outcrop at the southern and northern slopes
138 (Fig.1) (El Gh'mari, 1995; Fichter et al., 1998). The gneiss is enriched in Mg mainly because of the
139 presence of biotite and chlorite (El Gh'mari, 1995; Fichter, 1997). Hydrothermal processes caused
140 the alteration and transformation of albite, K-feldspar and muscovite into fine-grained illite and
141 quartz; biotite and albite disappeared to a large extent. The strongly altered granite (on the northern
142 slope) is characterized by larger amounts of quartz, clays and Fe-oxides, small amounts of apatite
143 ($<1\%$), and by higher Mg but lower Ca, K and Na contents than the less altered granite at the
144 southern slope (El Gh'mari, 1995; Fichter et al., 1998). In addition, the northern sun-facing slope is
145 characterized by a drier and slightly warmer climate with 10% less precipitation than observed for
146 the southern slope. The soils are brown acidic to ochreous brown podzolic and are generally about 1
147 meter thick. They are very coarse grained, sandy and rich in gravel (Fichter et al., 1998). The brown
148 acidic soils are mainly located on the northern slope and are characterized by higher clay contents,
149 lower K-feldspar, lower albite, higher cation exchange capacity (CEC), lower pH and lower organic
150 matter content than the ochreous brown podzolic soils, which are mainly located on the southern
151 slope (Fichter 1997; Fichter et al., 1998). The pedological differences are due to the different
152 mineralogical compositions of the northern and southern bedrocks, and the different types of
153 vegetation but also the different orientations of the slopes. Indeed, exposure and consequently
154 rainfall and temperature influence the chemical weathering of soils and organic matter, the soil
155 acidity and processes of clay formation (Egli et al., 2007; 2010).

156 A sandy saprolite separates soil and granite. Its thickness varies between 1 and 9 meters; on the
157 southern slope it is generally thicker (El Gh'Mari, 1995) with the most important thickness in the
158 depression zone near the four springs CS1, CS2, CS3 and CS4. The forest covers 90% of the area
159 and corresponds to about 80% spruce (mainly *Piceas Abies L.*) and 20% beech (*Fagus Sylvatica*).
160 The catchment contains 10 different springs feeding the Strengbach streamlet (Fig.1).
161 The catchment is situated in a remote area lacking direct industrial activities. Nevertheless,
162 atmospheric pollution occurs in many forms (acidic deposition, O₃ pollution or as atmospheric dust
163 deposition). Anthropogenic Pb has been identified in the atmospheric dust depositions and soils
164 (Lahd Geagea et al., 2008b; Stille et al., 2011). The forestry has increased the proportion of spruce
165 with especially dense spruce plots planted between 1890 and 1960. The site is well equipped for
166 sampling of atmospheric depositions and spring and stream waters at the whole catchment scale.
167 For this study, the stream and the different springs of the catchment were collected at various
168 hydrological periods with high and low water levels during a two years period (2004-2006) in order
169 to obtain a precise chemical and isotopic signature of the different sources in this hydrological
170 system (Fig. 1). The springs SG, ARG, RH, BH, CS₃ and CS₄ are located on the northern slope and
171 the springs CS₁, CS₂, SH and RUZS emerge at the southern slope (Fig. 1). The spring RUZS is
172 situated in the humid zone at the bottom of the catchment near the outlet (saturated area, Fig.1) and
173 covered by dense grass vegetation. In addition rain (bulk precipitation) and throughfalls were
174 collected using rain collectors and gutters, respectively.

175

176 **3. Analytical procedures**

177 The different spring waters were collected every 6 weeks during 2 years unless the springs were dry
178 or under snow. The waters were collected in clean polyethylene (HDPE) bottles (250 ml for major
179 element analysis and 1 liter for isotope and trace element analysis) and filtered the same day
180 through a 0.45 μ m pore diameter membrane (Millipore ester cellulose, 142 mm diameter). Before,
181 the HDPE bottles were washed with HCl 10% (24h contact) and then rinsed with MilliQ deionised

182 water. The filtrated waters for trace element and U-Sr isotopic composition determinations were
183 acidified with 250 μ l of ultrapure HNO₃ 13M and then stored in a cold room at 5°C.

184 The pH were measured just after filtration using a pHM210 MeterLab (Radiometer analytical) with
185 an Mettler HA405-DXKS8 electrode and calibrated with standard buffer solutions (pH 4.00 and
186 7.00 at 25°C). The precision of the pH measurement was \pm 0.02 units. The electrical conductivity
187 and the alkalinity were determined respectively using a CDM210 MeterLab (radiometer analytical)
188 with an CDC 745-9 electrode (precision 0.1 μ S/cm) and with 716DMS Titrino (Metrohm ; precision
189 of 0.01 meq/l – Acid/base titration, Gran method).

190 The major element contents were determined by ionic chromatography, atomic absorption,
191 colorimetry and ICP-AES and the trace element concentrations were determined by ICP-MS
192 (Pierret et al., 2010, Chabaux et al., 2011). The analytical uncertainty of the major cation and anion
193 determinations in solution (by atomic absorption and ionic chromatography Dionex, 4000 I) is \pm 2
194 %. The uncertainty on the major element concentrations such as Fe, Al, Mn and Si (by ICP-EAS,
195 Jobin Yvon 124) is \pm 5%, and that of the trace element concentrations (by ICP-MS, VG Plasma
196 Quad; Thermo Electron) is \pm 5%. The dissolved organic carbon (DOC) was determined using an
197 organic carbon analyser (Shimadzu TOC-5000A) with an uncertainty of 5 to 10 %, The accuracy of
198 the analysis was assessed by regular analysis of the SLRS-4 riverine standards,

199 The Sr isotopic ratios were determined by thermo-ionisation mass spectrometry on a multi-collector
200 VG-Sector mass spectrometer. Sr was extracted by standard procedures (Steinmann et Stille, 1997;
201 Lahd Geagea et al., 2008a; Pierret et al., 2010). The routinely measured NBS 987 standard yield an
202 average ⁸⁷Sr/⁸⁶Sr ratio of 0.71026 ± 0.00002 (2s) for 10 determinations during the course of this
203 study. The U isotope ratios were analysed on a TRITON Thermofinnigan mass spectrometer after
204 separation and purification of U by anionic exchange chromatography (resin AG1X8, 200-400
205 mesh) following the classical technique used in the lab (e.g. Chabaux et al., 1997; Pelt et al., 2008,
206 Pierret et al., 2012). During this study (2006-2008) the reproducibility of the U isotopic analyses

207 was tested with the HU1 standard which yield an average value of 0.999 ± 0.004 (2σ) ($n=27$). The
208 analytical error for the ($^{234}\text{U}/^{238}\text{U}$) activity ratio is $\pm 0.5\%$ (2σ).

209

210 **4. Results**

211 Previous studies performed on the Strengbach watershed mainly focused on the geochemical and
212 isotopic variations of dissolved loads of the stream waters collected at its outlet. The new results
213 (Tables 1 and 2) yield a first complete dataset of the spatial variability of major and trace element
214 concentrations as well as Sr and U isotope ratios of the spring and streamlet waters emerging on the
215 Strengbach watershed. The data also allow us to present the geochemical variability of the source as
216 well as stream waters at the outlet of the watershed over the period 2004-2006, that is to say during
217 two hydrologic cycles.

218

219 **4.1. The major and trace element data**

220 Among the spring and stream waters the pH, alkalinity, DOC, TDSw (total dissolved solids, table
221 1), TDS-Ca (total dissolved solids-cation; table 1) and conductivity are highly variable and range
222 respectively from 5 to 6.85, from 0 to 0.16 meq/L, from 0.42 to 11.6 ppm, from 10.3 to 26.8 mg/L,
223 from 3.87 to 9.05 mg/L, and from 13.2 to 60.3 $\mu\text{S}/\text{cm}$ (Table 1). The pH is well correlated with
224 alkalinity and TDS-Ca (Fig. 2). The range of variations of the major element concentrations at the
225 watershed scale can be important but clearly depends on the chemical elements and the physico-
226 chemical parameters. For the cation concentrations the variation at the watershed scale reaches
227 about one order of magnitude for Mg, but only 20 to 30% for Na concentrations. At the watershed
228 scale, the most discriminating cation is Mg. SH and CS₁ sources are marked by weakest Mg and Ca
229 and the SG source by highest concentrations (Table 1). In addition, as illustrated by Ca/Na, Mg/Na
230 and $\text{H}_4\text{SiO}_4/\text{Ca}$ concentration ratios (Fig.3) but also the K/Na, Sr/Na, Mg/Ca ratios (not shown), the
231 different springs are not only marked by different mean major element concentrations (2004-2006
232 period) but also by different elemental ratios.

233 The data points of the different sources define linear trends with slopes different from each other
234 (Fig. 3). The variation of the Ca/Na and Mg/Na ratios are much larger at the watershed scale than at
235 the scale of a single spring. On the basis of the above data a clear distinction is possible between the
236 spring waters from the northern slope (SG, RH, ARG, CS₃, CS₄ and BH) and those from the
237 southern slope (CS₁, CS₂, SH and RUZS), the former being characterized by higher pH, alkalinity,
238 conductivity TDSw and Ca/Na, K/Na and Mg/Na ratios than the latter (Figs. 2 and 3; table 1). In
239 addition to the spatial variations, the chemical signatures of waters also show temporal variations.
240 These are strongest for the most DOC enriched sources (RUZS, SH) and for the stream at the outlet
241 (RS).

242

243 **4.2. Sr and U isotope data**

244 The ⁸⁷Sr/⁸⁶Sr isotopic composition values of the different spring waters are highly variable and
245 range between 0.72206 (RH) and 0.72801 (SH) with an average Sr isotopic composition for the
246 stream at the outlet of 0.72573 (Fig. 4, Table 1). The data show a clear relationship between the Sr
247 isotopic signature and the geographical location in the watershed; the springs from the northern
248 slope are characterized by lower ⁸⁷Sr/⁸⁶Sr ratios and higher Sr concentrations (Fig. 4).

249 As shown in Fig.6, the variation range of (²³⁴U/²³⁸U) AR in the source waters is much larger than
250 that of the streamlets waters at the outlet. The U AR range from 1.112 (BH) to 0.819 (CS3); the
251 average (²³⁴U/²³⁸U) AR for the stream at the outlet is 1.104. Among the 9 springs analyzed, 8 of
252 them have unusual low (²³⁴U/²³⁸U) AR <1. In addition, and to the best of our knowledge, these
253 values are the lowest ever published before for superficial waters. Indeed, the U AR measured in
254 world surface rivers or groundwaters have generally (²³⁴U/²³⁸U) >1 (see introduction and citations
255 therein).

256 In contrast to Sr isotopic compositions (Fig. 6) or chemical concentrations (Fig. 3) (²³⁴U/²³⁸U) AR
257 of a single source do not significantly vary over the period 2004-2006 (Fig 7). Finally, ⁸⁷Sr/⁸⁶Sr and
258 ²³⁴U/²³⁸U AR of the source waters are not correlated with each other and in contrast to the Sr

259 isotopic compositions or chemical concentrations (Fig 6) there is no clear distinction between the U
260 AR of the springs from the southern and northern slope. In the Strengbach watershed there is a clear
261 increase of the U AR of the source waters when the altitude of the spring decreases. A similar
262 behavior has been observed for waters from another small granitic watershed in the Vosges
263 Mountain, the Ringelbach watershed (Schaffhauser et al., 2014). But in contrast to the Ringelbach
264 catchment, where the U AR in the spring waters are above 1, one observed for the spring waters of
265 the Strengbach catchment $U\ AR \leq 1$ except for BH source.

266

267 **5. Discussion**

268

269 **5.1 Geochemical and Sr isotopic characteristics of the spring waters:**

270 As shown in the result section, the chemical characteristics of the sources are marked by an
271 important spatial variation with in particular a clear distinction between the springs from the
272 northern and the southern slope (Fig. 3), It appears that the Ca/Na, Mg/Na, and H_4SiO_4/Na
273 concentration ratios are neither rainwater nor throughfall controlled. Indeed rainwater and
274 throughfall show rather large variations of their Ca/Na or Mg/Na ratios (throughfall: Ca/Na: 0.9-
275 2.1; Mg/Na: 0.3-0.6) and do not plot at one of the extremities of the correlations. Mass balance
276 calculations show that the atmospheric input (including rain and throughfalls) corresponds to various
277 proportion of the exportation flux at the watershed scale, depending on type of element, as for
278 example 2%, 8% or 19 % for Si, U or Sr respectively (Table 3).

279 Similarly, the observation of a clear increase of the Sr isotope ratios with increasing discharge
280 towards values different from those of rainwater and/or throughfall Sr isotopic composition values
281 ($^{87}Sr/^{86}Sr$ ratios of 0.71110, 0.71327 and 0.71293 for rain, throughfall under spruces and throughfall
282 under beeches respectively) implies that rainwater or throughfall cannot be a significant source of
283 cation fluxes in the spring waters (Figs.7a and c and 13).

284 Therefore, chemical differences among the sources of the Strengbach watershed have to be
285 interpreted in terms of variations in the nature or in the intensity of water-rock interactions
286 occurring from one source to another or in the intensity of the interactions between different water
287 reservoirs. This interpretation is entirely consistent with the correlations observed for the spring
288 waters at the watershed scale between the alkalinity, TDS_w and their pH (Fig. 2; Table 1), since
289 consumption of H⁺ during silicate weathering increases pH and alkalinity. Thus, from these data it
290 appears, that the spring waters from the northern slope with higher total dissolved solid contents,
291 higher alkalinity and pH values (SG, CS4, CS3, RH with BH having the highest values) are more
292 involved in weathering reactions, or are subject to more intense weathering processes than spring
293 waters from the southern slope (especially SH, RUZS and CS1).

294 The geochemical signatures of the different springs can be generally linked to specific lithological
295 and mineralogical differences existing for the two hillsides of the catchment. This is particularly
296 obvious for the SG spring, which emerges near the top of the catchment, just below the gneiss,
297 whereas the other sources emerge within the granitic environment (Fig. 1). In comparison with the
298 granite, the gneiss has 4 to 5 times higher Mg concentrations due to important occurrences of biotite
299 and chlorite (El Gh'mari, 1995; Table 4). The Mg/Na and Mg/Ca elemental ratios are about 7.5
300 respectively 11 for the gneiss and range from 0.7 to 0.1 respectively 0.5 to 1.5 for the granite (El
301 Gh'Mari, 1995; Fichter, 1997; Table 4). Mg is also more concentrated in the gneiss-derived soils
302 (MgO : 0.9 to 1.4 wt.%), than in other soil profiles of the catchment (0.4 to 0.7 wt.%) (El Gh'Mari,
303 1995; Lefèvre, 1988; Table 4). Similarly, the Ca/Na ratios of the gneiss (0.71) and the
304 corresponding soils (0.7 to 9.2) are higher than those of the granite (0.2 to 0.6) or of the
305 corresponding soils (0.1 to 0.5) (El Gh'Mari, 1995; Fichter, 1997; Table 4). All these lithological
306 and pedological characteristics explain why the SG spring waters are more enriched in Mg and have
307 higher Mg/Ca, Mg/Na and Ca/Na ratios than the other springs (Fig. 3).

308 The variation of the chemical data of the other spring waters emerging from the granite might result
309 from the specific characteristics of the two hillsides, which show different types and thicknesses of

310 soils and saprolite and different degrees of hydrothermal alteration of the granitic bedrock (Lefèvre,
311 1988; Fichter, 1997; El Gh'Mari, 1998; see also geological setting). Indeed, the study of 13
312 weathering profiles from the whole Strengbach catchment point to important variations of the
313 mineralogical composition of soils and bedrocks at the catchment scale (El Gh'Mari, 1995; Fichter,
314 1997; Aubert 2001; Prunier, 2008; Stille et al. 2009). The soils from the northern slope are brown
315 acidic and overlay a 0.5 to 4 m thick saprolite. At the southern slope, however, an ochreous
316 podzolic soil type overlays a much thicker 4 to 9 m deep saprolite (El Gh'mari, 1995; Fichter et al.,
317 1998). The bedrock from the northern slope was subjected to stronger hydrothermal alteration,
318 which caused disappearance of albite and biotite, diminution of K-feldspar but an increase of
319 quartz, clays and white mica contents and the occurrence of hematite (Bonneau, 1994; Fichter,
320 1997; El Gh'Mari, 1995). The hydrothermally strongly altered granite on the northern slope is
321 characterized by generally higher Mg and lower Ca and Na contents than observed for the less
322 altered granite on the southern slope (Fichter et al., 1998. El Gh'Mari, 1995; Table 4). This could
323 account for the comparatively higher Mg concentrations and Mg/Na ratios of the sources from the
324 northern slope, but not for e.g. the higher Ca or K concentrations.

325 The $^{87}\text{Sr}/^{86}\text{Sr}$ ratios of springs from the southern slope (SH, CS₂, CS₁, RUZS) are, like the
326 corresponding rocks and soils (Aubert et al. 2002) (Fig. 7), more radiogenic with lower Sr
327 concentrations than those from the northern slope (BH, RH, SG, CS₃, CS₄) (Fig. 4). Thus, the Sr
328 isotopic compositions of springs can be directly related to the signatures of the weathering profile
329 and their geographical localization. But the mineral phases involved in the weathering processes
330 and causing the geochemical characteristics of these superficial waters are still matter of discussion.

331 Based on Sr and Nd isotope ratios, Aubert et al. (2001) explained the isotopic signature of the
332 Strengbach stream water by mixing of two isotopically different end-members: apatite and
333 plagioclase. However, the Mg/Sr and Mg/Ca ratios of the waters cannot simply be explained by
334 dissolution of apatite and plagioclase (Fig. 8a,b). In addition, biotite and muscovite have far too
335 high Sr isotopic ratios (respectively 5.8 and 5.4; Aubert et al., 2001) and thus their contribution can

336 be ignored. The clay fractions, extracted from the two weathering profiles at sites HP and VP
337 (Prunier, 2008) can represent an end-member able to explain the Sr isotopic composition as well as
338 the Mg/Ca and Mg/Sr ratios of springs. The springs, bulk soils and clays from the southern slope
339 show higher $^{87}\text{Sr}/^{86}\text{Sr}$ ratios than those from the northern slope. Clay fraction contents in weathering
340 profiles from northern slope are twice as big as those from the southern slope. This suggests that the
341 impact of clay on the chemical composition of springs and streams is more important on the
342 northern than the southern slope. This also explains why the springs from the northern slope are
343 more radiogenic (Fig. 4a and b) with comparatively higher Mg/Ca and Mg/Sr ratios (Fig. 8a and b)
344 than those from southern slope.

345 Such an interpretation is consistent with results of numerical modeling, which indicates that
346 precipitation/dissolution of more or less crystallized clay minerals (such as smectite) control the Mg
347 concentrations and possibly the high Mg/Ca ratios in the source waters of the Strengbach watershed
348 (Godderis et al. 2006; 2009). The same authors proposed that Mg^{2+} is controlled by smectites, Ca^{2+}
349 by the dissolution of apatite and by smectite, and K^+ by smectite/illite precipitation and dissolution
350 of K-feldspar. Interaction with clays might occur all along the circulation pathway of waters in
351 soils, saprolite and in bedrock fractures. Recent studies in the Mule Hole watershed, Mackenzie
352 basin and Damma Glacier catchment confirm the importance of secondary mineral formation,
353 especially montmorillonite in the control of chemical composition of stream water at the watershed
354 scale (Violette et al., 2010; Beaulieu et al., 2011; Hindshaw et al., 2011).

355 Thus, the variation of the current chemical compositions of the source waters in the Strengbach
356 catchment possibly reflects dissolution/precipitation processes of secondary mineral phases like
357 clay minerals. In such a model the low apatite-like Sr isotopic composition values of the source
358 waters and comparatively high and not apatite-like Mg/Ca ratios can be explained by the fact that
359 the Sr has not been remobilized by alteration of primary apatite but by weathering of secondary
360 mineral phases, which integrated during an earlier stage of alteration and crystallization apatite-

361 derived Sr. At this point we therefore propose that the alteration flux controlling the $^{87}\text{Sr}/^{86}\text{Sr}$ and
362 Mg/Ca (resp Mg/Sr) variation in the sources is imposed by secondary minerals.

363

364 **5.2. $^{234}\text{U}/^{238}\text{U}$ AR in spring waters**

365 Observation of ($^{234}\text{U}/^{238}\text{U}$) AR < 1 in most of the spring and stream waters of the Strengbach
366 catchment is unusual as river waters exhibit generally ^{234}U excess (e.g., Chabaux et al., 2003). U AR
367 < 1 have already been observed for waters from the outlet of the Strengbach catchment (0.963 to
368 1.023) with a decrease of the U AR in the dissolved load when the discharge increases (Riotte et al.,
369 1999). The authors explained this variation by the involvement of different weathered end-
370 members: a water body enriched in ^{234}U which weathered the granitic bedrock at secular
371 equilibrium and waters with a U AR below unity representing mobilization of U from material that
372 has already been weathered. Our study shows an even larger range of variation of the U AR among
373 the different springs ranging from 0.819 (CS3) to 1.112 (BH) (Table 2). The lack of correlation
374 between ($^{234}\text{U}/^{238}\text{U}$) AR and $^{87}\text{Sr}/^{86}\text{Sr}$ isotopic compositions or chemical values (Fig. 5a and b) show
375 that AR are not simply lithology controlled.

376 The mechanisms classically involved to explain ($^{234}\text{U}/^{238}\text{U}$) AR >1 in natural waters are linked to the
377 recoil process associated to the decay of ^{238}U : 1) due to alpha recoil when ^{238}U decays to ^{234}Th , it can
378 be ejected out of a grain into the fluid if the distance to the grain boundary is smaller than the recoil
379 range of ^{234}Th (~30 nm; DePaolo et al., 2006); the ^{234}Th decays then rapidly to ^{234}U (^{234}Th half-life is
380 24 days); (2) α - particles emitted during radioactive decay damage the crystal lattice of mineral
381 grains and the recoil nuclide is subsequently easily mobilized out of the damaged site. As a
382 consequence, the daughter nuclide ^{234}U is preferentially leached relative to the parent ^{238}U during
383 weathering. Thus, natural waters with ($^{234}\text{U}/^{238}\text{U}$) AR < 1 most likely correspond to environments,
384 which have already experienced a loss of ^{234}U .

385 One might simply suggest that the U AR < 1 in the Strengbach source waters are the results of
386 circulation through already weathered soils, supposedly having U AR < 1 due to previous

387 weathering. However, chemical flux balance calculations show that the annual U fluxes from the
388 soils under spruces or beech trees represent at maximum about 8% or 22%, respectively, of the
389 annual U flux at the outlet (Table 3). At the same time, the U concentrations in the different
390 springs can reach on average 0.345 ppb whereas they range only between 0.011 to 0.023 ppb
391 (factor of 30 to 15 lower) in the deep soil solutions of the two experimental plots (Table 2). In
392 addition, ($^{234}\text{U}/^{238}\text{U}$) AR determined on soil solutions from depths between 5 and 70 cm, range from
393 0.899 and 0.945 under spruces and from 0.953 to 1.194 under beech trees (Prunier, 2008) whereas
394 they are significantly low for some spring waters (0.82). This indicates that circulations and
395 interactions in the saprolite and bedrock (below the soil) control the U isotopic signature in
396 spring and stream waters.

397 The relationship between the U AR and the altitude of the springs (Fig. 9) indicates that the springs
398 from both slopes with the lower U AR (CS1, CS2, CS3, CS4) are located at higher altitude and
399 circulate in zones where the saprolite reaches 7 to 9 m depth (El'Ghmari, 1995) than springs with
400 high U AR. The spring BH, with the highest U AR is located at the bottom of the watershed where
401 the saprolite layer reaches less than 1.5 m thickness (Fig. 1). Also RUZS was taken at low altitude
402 (950masl), but drains the whole wetland and, therefore, integrated an intermediate U AR. Thus, a
403 possible scenario explaining the ($^{234}\text{U}/^{238}\text{U}$) AR of the spring waters is that BH like sources are
404 closer to the "fresh" granite and reflect meteoric alteration of fresher rock material at secular
405 equilibrium, CS₁, CS₃, CS₂, CS₄ and SH sources, by contrast, drain thicker saprolite profiles and/or
406 less fresh granite and, therefore, their low AR may point to the mobilization of U from mineral
407 phases whose outermost surfaces have already been depleted in ^{234}U due to previous water-rock
408 interactions (old saprolite where the pool of excess ^{234}U has been exhausted). We therefore propose
409 that the $^{234}\text{U}/^{238}\text{U}$ AR in the catchments spring waters can be interpreted as a function of water
410 pathways. The sources emerging at high altitude, with AR<1, have circulated through already
411 weathered horizons (saprolite, fractured bedrock depleted in ^{234}U , i.e., with U AR <<1), whereas the
412 springs emerging at the bottom of the watershed have U AR>1 because of the interaction with

413 fresher mineral phases. Therefore, U disequilibrium ratios can be a powerful tool to study the water
414 pathways. These preferential flow paths cross more or less weathered materials implying various
415 ($^{234}\text{U}/^{238}\text{U}$) AR for the corresponding springs.

416 This interpretation is in agreement with a granite leaching experiment under continuous flow
417 through a reactor (Andersen et al., 2009). It has indeed been shown that during the experiment
418 (1200 hours) there is a clear trend of variation of the U AR in the outflowing waters, with
419 ($^{234}\text{U}/^{238}\text{U}$) AR >1 at the beginning of the experiment and a minimal value of 0.9 after 650 to 700
420 hours; then, the AR increased up to 0.95. The values suggest that at the beginning of the experiment
421 high exposure of fresh material promotes direct recoil of ^{234}U into water and potentially enhances
422 preferential release of ^{234}U from damaged lattice sites. However, since there was no renewal of
423 material, because the excess ^{234}U constitutes a finite pool of easy leachable ^{234}U , the ($^{234}\text{U}/^{238}\text{U}$)
424 values become lower than unity when this pool is used up.

425 Similarly, the observed ($^{234}\text{U}/^{238}\text{U}$) AR <1 in Strengbach springs might indicate that the rate of
426 production of ^{234}U excess (by direct recoil and preferential release) is lower than the rate of renewal
427 of material. This can be explained by continuous preferential water circulation along fractures (Le
428 Borgne et al., 2007), on old weathered mineral surfaces where the production of ^{234}U excess is
429 supposed to be low.

430 However, the springs emerging at lower altitude (mainly BH and to a lesser extent RH), with
431 ($^{234}\text{U}/^{238}\text{U}$) >1, circulate through fresher granite where α -recoil tracks have direct contact with the
432 outer mineral surfaces and thus with fresh mineral phases (Andersen et al., 2009).

433 At this point it is interesting to note that in a neighbored granite catchment (Ringelbach watershed)
434 all the sources only display U AR >1 (Schaffhauser, 2013; Schaffhauser et al., 2014). This small
435 catchment located in the Vosges massif at altitudes between 750 and 1100m (0.36 km²) also
436 consists of Hercynian granite capped in its upper part by residual Triassic sandstones (Schaffhauser
437 et al., 2014).

438 Plotting the U AR of springs of the both watersheds versus alkalinity and pH (Fig. 10) one observes
439 a good correlation where springs with highest U AR are characterized by highest alkalinity and pH
440 values. These two parameters can be considered to reflect the intensity of weathering and
441 water/rock interactions, meaning that the waters from the Ringelbach watershed are characterized
442 by more intense weathering. Only SG spring from the Strengbach catchment shows a slightly
443 different behavior because it originates from a gneiss and not a granite body (see section 5.1). The
444 modeling of chemical composition of the waters from the Ringelbach catchment implies mainly
445 dissolution of primary granite minerals and precipitation of secondary phases such as clays
446 (Schaffauser, 2013). Ringelbach stream waters present higher alkalinity, pH (Fig. 10) and also
447 conductivity, K, Mg, Si and Ca concentrations (not show) than spring and stream waters from
448 Strengbach watershed, which might point to higher dissolution processes. Thus, we suggest that the
449 waters with the lowest U AR correspond to less intense weathering in an already rock altered
450 system with only a few fresh and primary mineral phases whereas higher U AR correspond to more
451 intense weathering for waters circulating for example in fresher bedrock. In this way, the
452 weathering history might be older for the Strengbach watershed than the Ringelbach watershed.
453 This may be related to the fact that Triassic sandstones still cover the granite in the Ringelbach
454 catchment.

455 It is striking that the BH waters from Strengbach watershed plot in between the data from the
456 Strengbach and Ringelbach watershed (Fig. 10a and b) and are characterized by the highest pH
457 (6.7) and alkalinity despite the relatively high DOC content (2.27 ppm), which usually increases the
458 acidity of solution. If we consider that the proton inputs due to atmospheric deposition or biological
459 activity are homogeneous at the watershed scale, then the variations of pH in the different springs
460 only reflect water/rock interactions and the consumption of protons by dissolution reactions. The
461 high pH and alkalinity observed for the BH source are in this case consistent with the fact that its
462 water has interacted with fresher bedrock; this further implies a stronger weathering intensity and
463 higher dissolution rate of secondary phases such as smectite along the pathway of this source water.

464 In such a scenario, the relationship observed between ($^{234}\text{U}/^{238}\text{U}$) AR and Mg/Ca ratios (Fig. 11)
465 would indicate that the intensity or the nature of water reactions controlling the Ca-Mg budget of
466 these waters, namely the dissolution/precipitation reactions of Mg- or Ca-smectites (see discussion
467 in 5.1), would be clearly dependent on the weathering level of the saprolite/bedrock system. This is
468 consistent with the fact that 1) smectite occurs along the weathering profile and even in deep
469 weathering horizons (Fichter et al., 1998) and 2) the reactivity of secondary phases like smectite
470 control the chemistry of Mg and Ca in streamwater (this study, Godderis et al., 2006; 2009). In
471 addition, dissolution of clays implies an increase of Mg/Ca ratios in water (Fig. 8b). Thus, the
472 relation between U AR and Mg/Ca ratios for the Strengbach springs reflects nothing else than the
473 degree of alteration of the source rock being in contact with the waters: at low altitude the material
474 is fresher, the weathering intensity is more important (higher pH and alkalinity) and, thus, causes
475 higher Mg/Ca and U AR ratios in the waters than at higher altitudes.

476

477 **5.3. Temporal variations of spring waters**

478 The data obtained during 2 hydrological years allow for the analysis of the temporal variations of
479 the springs (Fig. 3). The spring RUZS shows the largest variations, which can be explained by the
480 fact that this spring drains wetland (10 to 15 % of the whole catchment area) with fluctuations in the
481 groundwater level and contributions.

482 The Sr isotopic compositions of single springs are correlated with discharge (Fig. 6a). In previous
483 studies these variations have been interpreted by mixing of superficial (soil solution type) and deep
484 (groundwater type) waters (Aubert et al., 2002). But, at the same time, the U AR show no temporal
485 variation and, therefore, no relation with discharge (Fig. 6b).

486 Consequently, the U AR and Sr isotopic compositions are not correlated. Similarly, there is no
487 correlation between U AR and geographical location and lithology (discussed in section 5.2). In
488 addition, the lack of temporal U AR variations indicates that the single springs are probably not the
489 result of mixing of different waters. In the same way, the lack of correlation between discharge and

490 DOC or NO₃, but also the majority of major and trace element concentrations suggests that the
491 variation of chemical composition of spring waters cannot be explained by a simple variation in the
492 contribution between different types of waters or as mixing between superficial waters (with high
493 DOC, NO₃ concentrations for instance) and deep waters. At the same time, the lack of correlation
494 between Sr isotopic compositions and concentrations for individual springs (Fig. 4a) confirms that
495 the temporal variations of spring waters cannot simply be explained by mixing between two end-
496 members (e.g. superficial and deep waters). The lack of variation of U AR in the individual springs
497 with changing discharge (Fig. 6) during 2 years further suggests that the water pathways are the
498 same whatever the hydrological conditions. Under these conditions, the water did not interact with
499 new fresh material but rather with minerals having experienced at their surface a prior loss of ²³⁴U
500 from damaged lattice sites (Andersen et al., 2009). In such a fractured bedrock system, the water
501 flow is often reduced to only a few main flow paths that control most of the hydrological response
502 of the aquifer (Le Borgne et al., 2007). These preferential flow paths along constant fractures in the
503 bedrocks might explain the homogeneous (²³⁴U/²³⁸U) AR of the different spring waters with time.
504 In contrast, there is a correlation between discharge and ⁸⁷Sr/⁸⁶Sr ratios for each single spring (Fig.
505 6b). With increasing discharge the Sr isotopic composition increases as well, whereas the Si
506 concentrations and alkalinity decrease (Fig. 12).
507 Different Si concentration-discharge relationships have been observed in several catchments and
508 three different types have been identified: type 1 when Si concentration decreases with discharge;
509 type 2 when Si concentration remains constant and type 3 when Si concentration remains constant
510 until a threshold in discharge is exceeded (Godsey et al., 2009; Maher, 2011). The springs from the
511 Strengbach watershed belong to the type 1 which are explained by average residence times shorter
512 than required to approach chemical equilibrium. Thus, the chemistry of waters could vary entirely
513 as a function of the nature of subsurface flow paths and the global solute fluxes depend strongly on
514 the geometry, relief, runoff and permeability of basins (Maher, 2011). In addition, the variation of
515 the Sr isotopic compositions with discharge suggests that the source of Sr changes with changing

516 hydrological condition; this confirms again that the temporal variation cannot be explained by a
517 mixing process but possibly by changing residence times of fluid and/or flow rate which according
518 to Maher (2010) have an important impact on the weathering rates. This is in accordance with the
519 hypothesis of preferential flow pathways through fractures for the water circulation in the basin.
520 In addition, modeling studies have shown that precipitation/dissolution process of secondary phases
521 control the dissolved Si export in stream waters (Godderis et al., 2006; Violette et al., 2010;
522 Beaulieu et al., 2011). Thus, the decrease of Si concentration with increasing discharge can be
523 explained by a change in the ratio between dissolution and precipitation of clays (see also chapter
524 5.2). We propose that at high discharge the water is undersaturated for clay precipitation (lower Si
525 concentration) causing a more important contribution by dissolution of clays as implied by the
526 higher Mg/Ca (see chapter 5.1) and Sr isotopic ratios (Fig. 11c). Thus, our study confirms that
527 hydrological properties limit the solute fluxes carried by rivers and physico-chemical conditions.

528

529 **5.4. The chemical and isotopic signatures of the waters at the Strengbach outlet**

530 The stream at the catchments outlet shows with increasing discharge increasing $^{87}\text{Sr}/^{86}\text{Sr}$ and
531 decreasing alkalinity, pH, H_4SiO_4 , and $(^{234}\text{U}/^{238}\text{U})$ AR (Fig. 13a-e). The important point is that the
532 variation of U AR observed at the outlet (Fig. 13e) can only be explained by a change in the
533 discharge contribution of the different springs because the U AR of single springs are constant with
534 time (Fig. 6). When the discharge increases, the U AR values tend towards 0.95, which is close to
535 the $(^{234}\text{U}/^{238}\text{U})$ AR of the spring from the saturated area (RUZS) (Figs. 6 and 14). Previous papers
536 proposed that during storm events, the contribution of the small saturated zone could reach up to 30
537 % of the runoff (Idir et al., 1999; Ladouche et al., 2001). Similarly, the increase of the Sr isotopic
538 composition with increasing discharge points to the important contribution of RUZS to the
539 streamlet during high discharge events (Fig. 13d).

540 However, during the lowest discharge, the U AR of the stream at the outlet is > 1 (max. 1.023).
541 These higher values can only be explained by a more important contribution of the spring BH from

542 the northern slope which is the only one with a U AR>1 (average: 1.103; Table 1; Fig.14). Other
543 parameters such as H_4SiO_4 , pH and alkalinity confirm the important contribution of the BH spring
544 to the streamlet during low discharge (Fig. 13). Similarly, the position of the RUZS spring with the
545 low pH, alkalinity and silica concentrations (Fig. 13) confirms its important contribution during
546 high discharge. But also the fact that the Sr isotopic composition of the stream at the outlet
547 decreases with decreasing discharge is in accordance with a more important contribution of the less
548 radiogenic springs from the northern (e.g. BH) (Fig. 13) than from the southern slope (Fig. 4).

549

550 **6. Conclusion :**

551 The study shows that the small Strengbach catchment drains different sources and streams with very
552 different isotopic and geochemical signatures. This heterogeneity is mainly related to:

553 - the parent material (gneiss, more or less hydrothermally altered granite) and the degree of their
554 weathering. This is confirmed by the fact that the sources draining the northern slope
555 (hydrothermally much more altered) have higher TDSw-, pH values, higher Ca, K, Mg
556 concentrations and lower $^{87}Sr/^{86}Sr$ ratios than sources draining the southern slope.

557 - the water flow is probably controlled by pathways through main fractures, as it is generally the
558 case in fractured granite systems.

559 This study has also shown, that there is an important decoupling between chemical composition on
560 the one hand and the $^{87}Sr/^{86}Sr$ ratios and ($^{234}U/^{238}U$) AR on the other hand. The Sr isotopic
561 compositions of the source waters are generally thought to be the result of alteration of primary
562 mineral phases such as apatite. However, the low apatite-like Sr isotopic composition but
563 comparatively high and not apatite-like Mg/Ca ratio cannot simply be derived from apatite
564 dissolution; however, they might originate from alteration of secondary mineral phases like clay
565 minerals, which integrated during their formation an apatite-derived Sr isotopic composition. The
566 dissolution and precipitation dynamics of secondary phases, especially clays such as
567 montmorillonite, seem to control the mobility of Si, Ca or Mg and, therefore, emphasize the key

568 role of the clays reactivity in the biogeochemical transfer of especially nutrient elements like Ca and
569 Mg.

570 Different processes control the variation of the U AR. Springs at high altitude with U AR<1 have
571 circulated through already weathered bedrock (thick saprolite and fractured rock) and have
572 interacted with already weathered surface minerals. These uncommon values for surface waters are
573 due to strong ^{234}U depletion during predating alteration processes of the bedrock granite. At the
574 opposite, springs emerging at the bottom of the watershed have U AR >1 because of interaction
575 with fresher materials.

576 The lack of variation of U AR in the individual springs with changing discharge during 2 years
577 suggests that the water pathways are the same whatever the hydrological conditions and that there is
578 no interaction between the different source waters.

579 It appears that the ($^{234}\text{U}/^{238}\text{U}$) AR is a very important tracer for studying and deciphering the
580 contribution of the different source fluxes at the catchment scale because this unique geochemical
581 parameter is different for each individual spring and at the same time remains unchanged for each
582 of the springs with changing discharge and fluctuating hydrological conditions. Without this
583 parameter it would not have been possible to decipher the real contribution of the different water
584 masses, especially that of the BH spring at low discharge conditions.

585 Thus all these observations converge toward the same functioning:

586 - The proportion of the contributions of the different springs to the stream at the outlet varies in
587 function of the hydrological conditions; the variable contributions of the different sources carrying
588 different geochemical signatures define the signature of the waters at the Strengbach outlet.

589 - During high flow events, the contribution of the saturated area (RUZS) to the streamlet increases.

590 - At low discharge, the contributions of springs from the northern slope become important (e.g.
591 BH).

592 The U-Sr isotope study, combined with physico-chemical investigations of the waters offered the
593 opportunity to better understand the processes causing the hydrochemical signature and its temporal

594 variation in each of the individual springs and in the stream waters at the outlet of the small
595 catchment. Indeed, this work points not only to the importance to investigate larger time intervals
596 including one total or even two hydrological cycles but also the interest of geographically enlarged
597 studies including several springs; punctual or only outlet observations will not allow for
598 understanding of the complex functioning of a watershed.

599 The study further highlights the important impact of different and independent water pathways in
600 fractured granite controlling the different geochemical and isotopic signatures of the waters.

601

602 **Acknowledgements**

603 We thank Daniel Million, Sophie Gangloff, Sylvain Bénarioumlil and René Boutin for technical
604 assistance. We would like to warmly acknowledge Yves Godd ris and Yann Lucas for discussion
605 about modeling. The manuscript benefit from constructive reviews from Stephan SK K hler and an
606 anonymous reviewer. The Observatoire Hydro-G ochimique de l'Environnement OHGE is
607 financially supported by INSU-CNRS, as well as by the REALISE network. This work has been
608 funding by EC2CO INSU CNRS program, and by 7th PCRD EU program (SoilTrec program). This
609 is an EOST contribution.

610

611

612 **References:**

613

- 614 Andersen M.B., Erel Y. and Bourdon B.: Experimental evidence for ^{234}U - ^{238}U fractionation during
615 granite weathering with implications for $^{234}\text{U}/^{238}\text{U}$ in natural waters. *Geochim. Cosmochim. Ac.*, 73.
616 4124-4141. 2009.
- 617 Andrews J.N. and Kay R.L.F.: The U contents and $^{234}\text{U}/^{238}\text{U}$ activity ratios of dissolved uranium in
618 groundwaters from some Triassic sandstones in England. *Isotope Geoscience* 1. 101-117. 1983.
- 619 Aubert D., Stille P. and Probst A.: REE fractionation during granite weathering and removal by
620 waters and suspended loads: Sr and Nd isotopic evidence. *Geochim. Cosmochim. Ac.* 65. 387-406.
621 2001.
- 622 Aubert D., Probst A., Stille P. and Viville D.: Evidence of hydrological control of Sr behavior in
623 stream water (Strengbach catchment, Vosges mountains, France). *Appl. Geochem.*, 17. 285-300.
624 2002.
- 625 Bagard M.L., Chabaux F., Pokrovsky O.S., Viers J., Prokushkin A.A., Stille P., Rihs S., Schmitt
626 A.D. and Dupré B.: Seasonal variability of element fluxes in two Central Siberian rivers draining
627 high latitude permafrost dominated areas. *Geochim. Cosmochim. Ac.*, 75. 3335-3357. 2011.
- 628 Berger T.W., Untersteiner H., Schume H. and Jost G.: Throughfall fluxes in a secondary spruce
629 (*Picea abies*), a beech (*Fagus sylvatica*) and a mixed spruce-beech stand. *For. Ecol. Manage.*, 255.
630 605-618. 2008.
- 631 Beaulieu E., Godderis Y., Labat D., Roelandt C., Calmels D. and Gaillardet J.: Modeling of water-
632 rock interaction in the Mackenzie basin: Competition between sulfuric and carbonic acids. *Chem.*
633 *Geol.*, 289. 114-123. 2011.
- 634 Bickle M.J., Chapman H.J., Bunbury J., Harris N.B.W., Fairchild I.J., Ahmad T. and Pomies C.:
635 Relative contributions of silicate and carbonate rocks to riverine Sr fluxes in the headwaters of the
636 Ganges. *Geochim. Cosmochim. Ac.*, 69. 2221-2240. 2005.

637 Blum J.D., Carey A.G., Jacobson A.D., and Chamberlain P.: Carbonate versus silicate weathering
638 in the Raikhot watershed within the High Himalayan Crystalline Series. *Geology*. 26. 411–414.
639 1998.

640 Blundy J. and Wood B.: Mineral-melt partitioning of uranium, thorium and their daughters. In :
641 *Uranium-Series Geochemistry*. 52. 59-123. 2003.

642 Bonotto D. M. and Andrews J. N.: The mechanism of $U\text{-}^{234}/U\text{-}^{238}$ activity ratio enhancement in
643 karstic limestone groundwater. *Chem. Geol.*. 103. 193–206. 1993.

644 Bonotto D.M., Andrews J.N.: The transfer of uranium isotopes ^{234}U and ^{238}U to the waters
645 interacting with carbonates from Mendip Hills area (England). *Appl. Radiat. Isotopes*. 52. 965-983.
646 2000.

647 Bourdon B., Bureau S., Andersen M.B., Pili E. and Hubert E.: Weathering rates from up to bottom
648 in carbonate environment. *Chem. Geol.*. 258. 275-287. 2009.

649 Boutin R., Montigny R. et Thuizat R.: Chronologie K-Ar et $^{39}\text{Ar}/^{40}\text{Ar}$ du métamorphisme et du
650 magmatisme des Vosges. Comparaison avec les massifs varisques avoisinants et détermination de
651 l'âge de la limite Viséen inférieur – viséen supérieur. *Geologie de la France* 1. 3-25. 1995.

652 Brantley S.L., Goldhaber M.B. and Ragnarsdottir V. K.: Crossing disciplines and scales to
653 understand the Critical Zone. *Elements*. 3. 307-314. 2008.

654 Brioshi L., Steinmann M., Lucot E., Pierret M.C., Stille P., Prunier J. and Badot P.M. : Transfer of
655 rare earth elements (REE) from natural soil to plant systems: implications for the environmental
656 availability of anthropogenic REE. *Plant Soil*. 366. 143-163. 2013.

657 Camacho A., Devesa R., Vallés I., Serrano I., Soler J., Blasquez S., Ortega X. and Matia L.:
658 Distribution of uranium isotopes in surface water of the Llobregat river basin (Northeast Spain). *J.*
659 *Environ. Radioactiv.*. 101. 1048-1054. 2010

660 Cenki Tok B., Chabaux F., Lemarchand D., Schmitt A.-D., Pierret M.-C., Viville D., Bagard M.-
661 L. and Stille P.: The impact of water-rock interaction and vegetation on calcium isotope

662 fractionation in soil- and stream waters of a small. forested catchment (the Strengbach case).
663 *Geochim. Cosmochim. Ac.*, 73. 2215-2228. 2009.

664 Chabaux. F., O'Nions. R.K., Cohen. A.S., Hein J.R.: ^{238}U - ^{234}U - ^{230}Th disequilibrium in Fe-Mn crusts :
665 Palaeoceanographic record or diagenetic alteration? *Geochim. Cosmoch. Ac.*, 61.. 3619-3632. 1997.

666 Chabaux. F., Riotte. J., Clauer. N. and France-Lanord. C.: Isotopic tracing of the dissolved U
667 fluxes in Himalayan rivers: implications for present and past U budgets of the Ganges-Brahmaputra
668 system *Geochim. Cosmoch. Ac.*, 65. 3201-3217. 2001.

669 Chabaux F., Riotte J., Dequincey O.: U-Th-Ra fractionation during weathering and river transport.
670 *Rev. Mineral. Geochem.*, 52. 533-576. 2003.

671 Chabaux. F., Riotte. J., Schmitt. A.-D., Carignan. J., Herckes. P., Pierret. M.-C.: Variations of U
672 and Sr isotope ratios in Alsace and Luxembourg rain waters: origin and hydrogeochemical
673 implications. *C. R. Geosci.*, 337. 1447-1456. 2005.

674 Chabaux. F., Bourdon. B., Riotte. J.: U-series Geochemistry in weathering profiles, river waters and
675 lakes. In : S. Krishnaswami and J.K. Cochran (Eds.). *U/Th Series Radionuclides in Aquatic
676 Systems*. Elsevier. Amsterdam. Radioactivity in the Environment. 13. 49-104. 2008.

677 Chabaux F., Granet M., Larque P., Riotte J., Skliarov E.V., Skliarova O., Alexeieva L., Risacher F.:
678 Geochemical and isotopic (Sr, U) variations of lake waters in the Ol'khon Region, Siberia, Russia:
679 Origin and paleoenvironmental implications. *C.R. Geosci.*, 343. 462-470. 2011.

680 Chen J.H., Edwards G.J., Wasserburg R.L.: ^{238}U - ^{234}U - ^{232}Th in seawater. *Earth Planet. Sci. Lett.*, 80.
681 241-251. 1986.

682 Cividini D., Lemarchand D., Boutin R., Pierret M-C., and Chabaux F.: From biological to
683 lithological control of the B geochemical cycle in a forested watershed (Strengbach, Vosges).
684 *Geochim. et Cosmochim. Ac.*, 74. 3143-3163. 2010.

685 Dambrine E., Le Goaster S., and Ranger J.: Croissance et nutrition minérale d'un peuplement
686 d'épicéa sur sol pauvre. II Prélèvement racinaire et transferts internes d'éléments minéraux au cours
687 de la croissance. *Ac. Œcol.*, 12. 791-808. 1991.

688 Dambrine E., Carisey N., Pollier B., and Granier A.: Effects of drought on the yellowing status and
689 the dynamic of mineral elements in the xylem sap of a declining spruce stand (*Picea abies* Karst.).
690 *Plant Soil*. 150. 303-306. 1992a.

691 Dambrine E., Pollier B., Poszwa A., Ranger J., Probst A., Viville D., Biron P. and Granier A.:
692 Evidence of current soil acidification in spruce (Strengbach catchment, Vosges mountains, North-
693 Eastern France). *Water, Air Soil Poll.* 105. 43-52. 1992b.

694 Degens E.T., Kempe S. and Richey J.E.: *Biogeochemistry of Major World Rivers*. Wiley, New
695 York. 356 pp., 1991.

696 DePaolo D., Maher K., Christensen J.N. and McManus J.: Sediment transport time measured with
697 U-series isotopes: Results from ODP North Atlantic drift site 984. *Earth and Planetary Science*
698 *Letters*. 248. 394-410. 2006.

699 DePaolo D., Lee V.E., Christensen J.N., and Maher K.: Uranium comminution ages: Sediment
700 transport and deposition time scales. *C.R. Geosci.* 344. 678-687. 2012.

701 Dosseto A., Bourdon B. and Turner S. P. : Uranium-series isotopes in river materials: insights into
702 the timescales of erosion and sediment transport. *Earth Planet. Sci Lett.* 265(1-2). 1-17. 2008.

703 Dosseto A., Buss H., Suresh P.O. : Rapid regolith formation over volcanic bedrock and implications
704 for landscape evolution. *Earth Planet. Sc. Lett.* 337-338. 47-55. 2012.

705 Dupré B., Dessert C., Oliva P., Goddérés Y., Viers J., François L., Millot R. and Gaillardet J.:
706 Rivers, chemical weathering and Earth's climate. *C.R. Geosciences*. 335. 1141-1160. 2003.

707 Durand S., Chabaux F., Rihs S., Düringer P. and Elsass P.: U isotope ratios as tracers of
708 groundwater inputs into surface waters: example of the Upper Rhine hydrosystem. *Chem. Geol.*
709 220. 1-19. 2005.

710 Egli. M., Mirabella. A., Sartori. G., Giacciai. D., Zanelli. R. & Plötze. M. : Effect of slope aspect on
711 transformation of clay minerals in Alpine soils. *Clay Minerals*. 42. 375-401. 2007.

712 Egli. M., Sartori. G. and Mirabella. A. : The effects of exposure and climate on the weathering of
713 late Pleistocene and Holocene Alpine soils. *Geomorph.* 114. 466-482. 2010

714 El Gh'Mari A.: Etude minéralogique, pétrophysique et géochimique de la dynamique d'altération
715 d'un granite soumis aux dépôts atmosphériques acides (Bassin versant du Strengbach, Vosges,
716 France) mécanismes, bilans et modélisations. PhD. Thesis. University Strasbourg. 202 p., 1995.

717 Engstrom E., Rodushkin I., Ingri J., Baxter D.C., Ecker F., Osterlund H. and Ohlander B.: Temporal
718 isotopic variations of dissolved silicon in a pristine boreal river. *Chem. Geol.* 271. 142-152. 2010.

719 Fichter J.: Minéralogie quantitative et flux d'éléments minéraux libérés par altération des minéraux
720 des sols dans deux écosystèmes sur granite (Bassin versant du Strengbach, Vosges). PhD thesis.
721 Univ. Henri Poincaré, Nancy I. 284 p., 1997.

722 Fichter J., Turpault M.P., Dambrine E., and Ranger J.: Mineral evolution of acid forest soils in the
723 Strengbach catchment (Vosges mountains, N-E France). *Geoderma*. 82. 315-340. 1998.

724 Gaillardet J., Dupré B., Louvat P., and Allègre C.J.: Global silicate weathering and CO₂
725 consumption rates deduced from the chemistry of the large rivers. *Chem. Geol.* 159. 3-30. 1999.

726 Goddérès Y., François L.M., Probst A., Schott J., Moncoulon D., Labat D. and Viville D.:
727 Modelling weathering processes at the catchment scale: The WITCH numerical model. *Geochim.*
728 *Cosmochim. Acta.* 70. 1128-1147. 2006.

729 Goddérès Y., Roelandt C., Schott J., Pierret M.C. and François L.: Towards an integrated model of
730 weathering, climate, and biospheric processes. *Rev. Mineral. Geochem.* 70. 411-434. 2009.

731 Godsey S.E., Kirchner J.W., Clow D.W.: Concentration-discharge relationships reflect chemostatic
732 characteristics of US catchments. *Hydrol. Process.* 23. 1844-1864. 2009.

733 Grzymko T.J., Marcantonio F., McKee B.A. and Stewart C.M.: Temporal variability of uranium
734 concentrations and ²³⁴U/²³⁸U activity ratios in the Mississippi river and its tributaries. *Chem. Geol.*
735 243. 344-356. 2007.

736 Hindshaw R.S., Tipper E.T., Reynolds B.C., Lemarchand E., Wiederhold J.G., Magnusson J.,
737 Bernasconi S.M., Kertzschar R., and Bourdon B.: Hydrological control of stream water chemistry

738 in a glacial catchment (Damma Glacier, Switzerland). *Chem. Geol.*, 285, 215–230. 2011.

739 Idir S., Probst A., Viville D. and Probst J.L.: Contribution des surfaces saturées et des versants aux
740 flux d'eau et d'éléments exportés en période de crue : tracage à l'aide du carbone organique dissous
741 et de la silice. Cas du petit bassin versant du Strengbach (Vosges, France). *C.R. Acad. Sci.*, 328, 89-
742 96. 1999.

743 Kohler S.J., Lidman F. and Laudon H. : Landscape types and pH control organic matter mediated
744 mobilization of Al, Fe, U and La in boreal catchments. *Geochim. Cosmochim. Acta.*, 135, 190-202.
745 2014.

746 Ladouche B., Probst A., Viville D., Idir S., Baqué D., Loubet M., Probst J.-L., and Bariac T.:
747 Hydrograph separation using isotopic, chemical and hydrological approaches (Strengbach
748 catchment, France). *J. Hydrol.*, 242, 255-274. 2001.

749 Lahd Geagea M., Stille P., Gauthier-Lafaye F. and Millet M.: Tracing of industrial aerosol sources
750 in an urban environment using Pb, Sr and Nd isotopes. *Env. Sci. and Technol.*, 42, 692-698. 2008a.

751 Lahd Geagea M., Stille P., Gauthier-Lafaye F., Perrone T. and Aubert D.: Baseline determination of
752 the atmospheric Pb, Sr and Nd isotopic composition of the Rhine Valley, Vosges Mountain
753 (France) and the Central Swiss Alps. *Appl. Geochim.*, 23, 1703-1714. 2008b.

754 Laudon H., Seibert J., Kohler S. and Bishop K. : Hydrological flow paths during snowmelt:
755 congruence between hydrometric measurements and oxygen 18 in meltwater, soil water, and runoff.
756 *Water Resour. Res.*, 40, 3102–3102. 2004.

757 Le Borgne T., Bour O., Riley M.S., Gouze P., Pezard P., Belghoul A., Lods G., Le Provost R.,
758 Greswell R.B., Ellis P.A., Isakov E. and Last B.J.: Comparison of alternative methodologies for
759 identifying and characterizing preferential flow paths in heterogeneous aquifers. *J. Hydrol.*, 345,
760 134-148. 2007.

761 Lefèvre Y.: Les sols du bassin d'Aubure. (Haut-Rhin): caractérisation et facteurs de répartition.
762 *Ann. Sci. For.*, 45, 417-422. 1988.

763 Lemarchand E., Chabaux F., Vigier N., Millot R., Pierret M.C. : Lithium isotopic behaviour in a
764 forested granitic catchment (Strengbach, Vosges Mountains, France). *Geochim. Cosmochim. Ac.*,
765 74, 4612-4628, 2010.

766 Lemarchand D., Cividini D., Turpault M.P., Chabaux F. : Boron isotopes in different grain size
767 fractions : Exploring past and present water-rock interaction from two soil profiles (Strengbach,
768 Vosges Mountain). *Geochim. Cosmochim. Ac.*, 98, 78-93, 2012.

769 Maher K., Steefel C.I., DePaolo D.J. and Viani B.E. : The mineral dissolution rate conundrum:
770 Insights from reactive transport modeling of U isotopes and pore fluid chemistry in marine
771 sediments. *Geochim. Cosmochim. Ac.*, 70, 337-363, 2006.

772 Maher K. : The dependence of chemical weathering rates on fluid residence time. *Earth and*
773 *Planetary Science Letters*, 294, 101-110, 2010.

774 Maher K. : The role of fluid residence time and topographic scale in determining chemical fluxes
775 from landscapes. *Earth and Planet. Sc. Lett.*, 312, 48-58, 2011.

776 Martin J.M. and Meybeck M. : Element mass-balance of material carried by major world rivers.
777 *Mar. Chem.*, 7, 173-206, 1979.

778 Millot R., Gaillardet J., Dupré B. and Allègre C.J.: Northern latitude chemical weathering rates:
779 Clues from the Mackenzie River Basin, Canada. *Geochim. Cosmochim. Ac.*, 67, 1305-1329, 2003.

780 Nègre P., Allègre C.J., Dupré B., and Lewin E.: Erosion sources determined by inversion of major
781 and trace element ratios in river water: the Congo Basin case. *Earth Planet. Sci. Lett.*, 20, 59-76,
782 1993.

783 Oliva P., Viers J., and Dupré B.: Chemical weathering in granitic environments. *Chem. Geol.*, 202,
784 225-256, 2003.

785 Osmond J.K. and Cowart J.B.: The theory and uses of natural uranium isotopic variations in
786 hydrology. *Atomic Energy Rev.*, 14, 621-679, 1976.

787 Osmond J.K., Cowart J.B.: Groundwater. In: *Uranium series disequilibrium – Applications to*
788 *environmental problems*. Ivanovich M. Harmon RS (eds) Oxford Science Publications, Oxford, p

789 202-245. 1982.

790 Osmond. J.K.. Ivanovich. M.: Uranium-series mobilisation and surface hydrology. In: Ivanovich.
791 M.. Harmon. R.S. (Eds.). Uranium-series Disequilibrium: Applications to Earth. Marine and
792 Environmental Sciences. second ed. Clarendon Press Oxford. 258-289. 1992.

793 Oster J.L.. Ibarra D.E.. Harris C.R. and Maher K.: Influence of eolian deposition and rainfall
794 amounts on the U-isotopic composition of soil water and soil minerals. Geochim. Cosmochim. Ac..
795 88. 146-166. 2012.

796 Paces J.B.. Ludwig K.R.. Peterman Z.E.. Neymark L.A.: $^{234}\text{U}/^{238}\text{U}$ evidence for local recharge and
797 patterns of ground-water flow in the vicinity of Yucca Mountain. Nevada. USA. Appl. Geochem..
798 17. 751-779. 2002.

799 Pelt E.. Chabaux F.. Innocent C.. Navarre-Sitchler A.L.. Sak P.B. and Brantley S.L.: Uranium-
800 thorium chronometry of weathering rinds: Rock alteration rate and paleo-isotopic record of
801 weathering fluids. Earth Planet. Sci. Lett.. 276. 98-105. 2008.

802 Pierret M.C.. Chabaux F.. Leroy S. and Causse C.: A record of Late Quaternary continental
803 weathering in the sediment of the Caspian Sea: evidence from U-Th. Sr isotopes. trace element and
804 palynological data. Quaternary Sci. Rev.. 51. 40-55. DOI 10. 1016/j.quascirev.2012.07.020. 2012.

805 Pierret M.C.. Bosch D.. Clauer N. and Blanc G.: Formation of metal-rich sediments in the Thetis
806 Deep (Red Sea) in the absence of brines : Implications for the genetic model. J. Geoch. Explor..
807 104. 12-26. DOI 10.1016/j.gexplo. 2009.

808 Probst A.. Dambrine E.. Viville D. and Fritz B.: Influence of acid atmospheric inputs on surface
809 water chemistry and mineral fluxes in a declining spruce stand within a small granitic catchment
810 (vosges massif- France). J. Hydrol.. 116. 101-124. 1990.

811 Probst A. Viville D. Fritz B. Ambroise B. and Dambrine E.: Hydrochemical budgets of a small
812 forested catchment exposed to acid deposition : the Strengbach catchment case study (Vosges
813 massif. France) W.A.S.P. 62. 337-347. 1992a.

814 Probst A., Fritz B., and Stille P.: Consequence of acid deposition on natural weathering processes:
815 field studies and modelling. In: Water Rock Interaction (Eds. Kharaka Y.K. and Maest A.S.)
816 Balkema/Rotterdam/ Brookfield. 581-584. 1992b.

817 Prunier J.: Etude du fonctionnement d'un écosystème forestier en climat tempéré. par l'apport de la
818 géochimie élémentaire et isotopique (Sr, U-Th-Ra). Cas du bassin versant du Strengbach (Vosges,
819 France). Thesis PhD. Uni. de Strasbourg. 303pp.. 2008.

820 Riotte J. and Chabaux F.: ($^{234}\text{U}/^{238}\text{U}$) activity ratios in freshwaters as tracers of hydrological
821 processes: the Strengbach watershed, Vosges, France. *Geochim. Cosmochim. Ac.*, 63. 1263-1275.
822 1999.

823 Riotte J., Chabaux F., Benedetti M., Dia A., Gérard M., Boulègue J., and Etamé J.: U colloidal
824 transport and origin of the ^{234}U - ^{238}U fractionation in surface waters : new insights from Mount
825 Cameroon. *Chem. Geol.*, 202. 365-381. 2003.

826 Schaffhauser T.: Traçage et modélisation des processus d'altération à l'échelle d'un petit bassin
827 versant, le Ringelbach (Vosges, France). Thesis PhD. Université de Strasbourg. 343pp. 2013.

828 Schaffhauser T., Chabaux F., Ambroise B., Lucas Y., Stille P., Perronne T., Fritz B.: Geochemical
829 and isotopic (U, Sr) tracing of water pathways in the small granitic Ringelbach research catchment
830 (Vosges Mountains, France). *Chem. Geol.*, 374. 117-127. 2014.

831 Steinmann M. and Stille P.: Controls on transport and fractionation of the rare earth elements in
832 stream water of a mixed basaltic-granitic catchment basin (Massif Central, France) *Chem. Geol.*,
833 254.1-18. 2009.

834 Stille P., Steinmann M., Pierret M.-C., Gauthier-Lafaye F., Chabaux F., Viville D., Pourcelot L.,
835 Matera V., Aouad G., and Aubert D.: The impact of vegetation on REE fractionation in stream
836 waters of a small forested catchment (the Strengbach case). *Geochim. Cosmochim. Ac.*, 70. 3217-
837 3230. 2006.

838 Stille P., Pierret M.-C., Steinmann M., Chabaux F., Boutin R., Aubert D., Pourcelot L., and Morvan

839 G.: Impact of atmospheric deposition. biogeochemical cycling and water-mineral interaction on
840 REE fractionation in acidic surface soils and soil water (the; Strengbach case). *Chem. Geol.* 264.
841 173-186. 2009.

842 Stille P., Pourcelot L., Granet M., Pierret M.-C., Perrone Th., Morvan G. and Chabaux F. :
843 Deposition and migration of atmospheric Pb in soils from a forested silicate catchment today and in
844 the past (Strengbach case ; Vosges mountains) ; evidence from ^{210}Pb activities and Pb isotope
845 ratios. *Chem. Geol.* 289. 140-153. 2011.

846 Stille P., Schmitt A.-D., Labolle F., Gangloff S., Cobert F., Lucot E., Pierret M.-C., Guéguen F.,
847 Brioschi L., Steinmann M., Chabaux F. : The suitability of annual growth rings as environmental
848 archives: Evidence from Sr, Nd, Pb and Ca isotopes in spruce growth rings (Strengbach case;
849 Vosges mountains, France). *CR Geosci.* 344. 297-311. 2012.

850 Stromman G., Rosseland B.O., Skipperud L., Burbkitbaev L.M., Uralbekov B., Heier L.S., Salbu
851 B.: Uranium activity ratio in water and fish from pit lakes in Kurday, Kazakhstan and Taboshar,
852 Tajikistan. *J. Environ. Radioactiv.* 1. 11. 2012.

853 Tipper E.T., Bickle M.J., Galy A., West A. J., Pomies C., and Chapman H.J.: The short term
854 climatic sensitivity of carbonate and silicate weathering fluxes: Insight from seasonal variations in
855 river chemistry. *Geochim. Cosmochim. Ac.* 70. 2337-2754. 2006.

856 Tricca A., Stille P., Steinmann M., Kiefel B., Samuel, J., and Eikenberg J. : Rare earth elements and
857 Sr and Nd isotopic compositions of dissolved and suspended loads from small river systems in the
858 Vosges mountains (France), the river Rhine and the groundwater. *Chem. Geol.* 160. 139-158. 1999.

859 Thimonier A., Schmitt M., Waldner P., and Schleppe P.: Seasonality of the Na/Cl ratio in
860 precipitation and implication of canopy leaching in validating chemical analyses of throughfall
861 samples. *Atmos. Environ.* 42. 9106-9117. 2008.

862 Ulrich, B.: Interaction of forest canopies with atmospheric constituents: SO₂, alkali and earth alkali
863 cations and chloride. In: Ulrich, B., Pankrath, J. (Eds.). *Effects of Accumulation of Air Pollutants in*
864 *Forest Ecosystems*. Reidel, Dordrecht. pp. 33–45. 1983.

865 Vigier N., Bourdon B., Turner S., and Allègre C.J.: Erosion timescales derived from U-decay series
866 measurements in rivers. *Earth Planet. Sci. Lett.*, 193, 549-563, 2001.

867 Vigier N., Burton K.W., Gilslason S.R., Rogers N.W., Duchon S., Thomas L., Hodge E., Schaefer
868 B.: The relationship between riverine U-series disequilibria and erosion rates in a basaltic terrain.
869 *Earth Planet. Sci. Lett.*, 249, 258-273, 2006.

870 Violette A., Godderis Y., Maréchal J.C., Riotte J., Oliva P., Mohan Kuma M.S., Sekhar M. and
871 Braun J.J. : Modelling the chemical weathering fluxes at the watershed scale in the Tropics (Mule
872 Hole, South India) : Relative contribution of the smectite/kaolinite assemblage versus primary
873 minerals. *Chem. Geol.*, 277, 42-60, 2010.

874 Viville D., Chabaux F., Stille P., Pierret M.C., Gangloff S.: Erosion and weathering fluxes in
875 granitic basins: The example of the Strengbach catchment (Vosges massif, eastern France). *Catena*,
876 92, 122-129, 2012.

877 Zakharova E.A., Pokrovsky O.S., Dupré B., Gaillardet J., Efimova L.E.: Chemical weathering of
878 silicate rocks in Karelia region and Kola peninsula, NW Russia: Assessing the effect of rock
879 composition, wetlands and vegetation. *Chem. Geol.*, 242, 255–277, 2007.

880

881

882

883

884

885

Discharge		pH	Cond.	Na ⁺	K ⁺	Mg ²⁺	Ca ²⁺	Alc	Cl ⁻	NO ₃ ⁻	SO ₄ ²⁻	DOC	H ₂ SiO ₄	Al	Mn	Fe	Ba	Rb	Sr	U	TDSw	TDS-ca	
date	ts	µS/cm	mmol/l	mmol/l	mmol/l	mmol/l	mmol/l	mmol/l	mmol/l	mmol/l	mmol/l	ppm	ppm	ppm	ppm	ppb	ppb	ppb	ppb	ppb	ppb	ppb	mg/l
Spring Collector CR	12/07/04	5.66	35.5	0.092	0.025	0.018	0.07	0.049	0.057	0.058	0.068	0.47	0.157	0.02	0.01	0.01	79.56	3.02	10.12	2.4	21.35	6.44	
CR	13/12/04	5.74	33.4	0.089	0.02	0.018	0.074	0.041	0.055	0.066	0.068	0.53	0.145	0.04	0.01	0.00	74.75	3.07	11.21	2.24	21.16	6.32	
CR	13/12/04	5.84	30.3	0.083	0.02	0.019	0.077	0.041	0.053	0.073	0.062	0.78	0.132	0.06	0.01	0.00	66.00	3.18	11.66	2.24	21.13	6.32	
CR	24/02/05	5.50	33.4	0.089	0.02	0.018	0.074	0.041	0.055	0.066	0.068	0.53	0.145	0.04	0.01	0.00	74.75	3.07	11.21	2.24	21.16	6.32	
CR	24/02/05	5.42	33.4	0.089	0.02	0.018	0.074	0.041	0.055	0.066	0.068	0.53	0.145	0.04	0.01	0.00	74.75	3.07	11.21	2.24	21.16	6.32	
CR	29/03/05	5.91	32.1	0.079	0.019	0.018	0.072	0.033	0.051	0.063	0.064	0.68	0.119	0.07	0.01	0.01	66.43	3.01	12.49	1.19	19.75	5.96	
CR	03/05/05	5.92	31.3	0.085	0.019	0.017	0.069	0.039	0.051	0.059	0.062	0.6	0.129	<0.01	0.00	0.05	73.47	2.42	10.12	1.14	19.84	6.00	
CR	31/05/05	5.92	31.3	0.085	0.019	0.017	0.069	0.039	0.051	0.059	0.062	0.6	0.129	<0.01	0.00	0.05	73.47	2.42	10.12	1.14	19.84	6.00	
CR	11/07/05	6.33	30.5	0.086	0.018	0.016	0.068	0.045	0.047	0.052	0.061	0.44	0.152	<0.01	0.00	0.04	83.05	2.82	11.40	1.15	19.37	5.93	
CR	22/08/05	6.49	29.9	0.092	0.018	0.017	0.071	0.041	0.051	0.063	0.063	0.5	0.159	0.05	0.01	0.01	74.37	2.85	10.21	1.23	20.39	6.15	
CR	03/09/05	6.39	30.9	0.089	0.018	0.016	0.069	0.045	0.049	0.052	0.063	0.53	0.153	0.02	0.01	0.01	73.77	3.17	11.91	1.23	20.97	6.15	
CR	07/02/06	6.38	31.8	0.092	0.017	0.017	0.073	0.035	0.050	0.060	0.064	0.62	0.154	0.04	0.01	0.01	76.68	3.03	11.00	1.22	21.19	6.30	
CR	03/03/07	6.05	31.4	0.075	0.017	0.017	0.073	0.045	0.049	0.055	0.064	0.64	0.154	0.06	0.01	0.01	69.27	3.01	11.66	1.22	21.63	6.30	
CR	10/07/06	6.05	31.4	0.075	0.017	0.017	0.073	0.045	0.049	0.055	0.064	0.64	0.154	0.06	0.01	0.01	69.27	3.01	11.66	1.22	21.63	6.30	
CR	21/08/06	6.12	30.0	0.084	0.018	0.017	0.065	0.039	0.049	0.059	0.059	0.59	0.137	nd	nd	nd	nd	nd	nd	nd	19.15	5.74	
CR	02/10/06	6.22	28.4	0.082	0.019	0.017	0.069	0.039	0.052	0.064	0.064	0.52	0.152	0.07	0.01	0.02	65.52	2.70	10.70	1.27	19.62	5.91	
CR	22/05/06	6.22	28.7	0.083	0.018	0.017	0.065	0.039	0.047	0.058	0.061	0.55	0.133	0.04	0.01	0.01	64.88	2.85	10.18	1.24	19.21	5.76	
CR	Average	6.15	31.61	0.086	0.019	0.017	0.070	0.041	0.052	0.061	0.062	0.67	0.140	0.04	0.01	0.01	73.21	2.90	11.16	1.20	21.14	6.07	
Spring C51	12/07/04	6.113	39.1	0.076	0.019	0.015	0.055	0.038	0.043	0.027	0.067	0.158	0.02	0.00	0.00	11.19	2.79	3.09	0.37	13.55	3.01		
C51	14/08/04	6.148	38.8	0.078	0.014	0.016	0.053	0.035	0.037	0.029	0.061	0.62	0.154	0.08	0.00	0.220	0.00	12.00	1.79	7.83	2.24	16.04	4.95
C51	13/12/04	6.318	6.12	24.5	0.073	0.013	0.014	0.048	0.02	0.039	0.027	0.027	0.87	0.145	0.11	0.026	0.005	11.11	2.69	7.71	0.37	11.52	4.55
C51	28/03/05	6.156	5.22	25.2	0.067	0.014	0.014	0.044	0.008	0.04	0.055	0.81	nd	0.120	0.19	0.037	0.002	14.73	2.82	8.81	0.38	14.14	4.27
C51	03/05/05	6.560	6.19	22.1	0.068	0.012	0.013	0.043	0.007	0.037	0.024	0.58	0.74	0.133	0.03	0.006	0.008	12.78	2.70	7.25	2.38	10.50	4.25
C51	31/05/05	6.268	6.33	24.0	0.072	0.014	0.014	0.051	0.035	0.036	0.022	0.657	0.74	0.138	<0.01	0.003	0.043	13.84	2.79	11.50	1.4	14.60	4.72
C51	11/07/05	6.076	6.48	23.5	0.067	0.014	0.014	0.053	0.042	0.036	0.024	0.550	0.64	0.157	0.03	0.004	0.029	13.84	2.85	9.54	0.19	15.85	4.88
C51	22/08/05	6.110	6.40	24.4	0.079	0.014	0.015	0.055	0.043	0.037	0.029	0.61	0.61	0.158	0.03	0.003	0.020	11.67	2.78	8.84	0.24	16.92	5.05
C51	03/09/05	6.192	6.50	24.0	0.075	0.014	0.015	0.049	0.029	0.046	0.026	0.588	0.66	0.151	0.04	0.023	0.000	12.66	2.78	8.73	0.15	15.27	4.69
C51	11/07/06	6.165	6.51	24.1	0.081	0.015	0.015	0.049	0.029	0.046	0.026	0.588	0.66	0.151	0.04	0.023	0.000	12.66	2.78	8.73	0.15	15.27	4.69
C51	03/04/06	6.172	6.33	25.5	0.068	0.015	0.015	0.044	0.028	0.044	0.038	0.62	1.76	0.113	0.26	0.044	0.015	17.94	2.86	8.54	0.53	14.64	4.37
C51	22/05/06	6.349	6.10	22.1	0.072	0.013	0.014	0.045	0.022	0.036	0.028	0.588	0.74	0.135	0.06	0.028	0.004	11.83	2.63	7.16	0.33	14.29	4.40
C51	10/02/06	6.062	6.04	23.6	0.075	0.014	0.014	0.047	0.037	0.048	0.022	0.587	0.63	0.151	0.01	0.021	0.000	19.29	2.47	7.72	0.19	14.69	4.55
C51	21/08/06	6.058	6.02	25.8	0.071	0.014	0.014	0.046	0.018	0.04	0.032	0.586	0.76	0.133	0.10	0.030	0.000	12.48	2.85	7.86	0.44	14.30	4.45
C51	02/10/06	6.035	5.85	25.7	0.071	0.013	0.014	0.044	0.014	0.044	0.033	0.657	0.78	0.135	0.12	0.032	0.000	14.07	2.75	8.31	0.51	14.24	4.33
C51	Average	6.06	6.24	25.2	0.074	0.014	0.014	0.047	0.037	0.048	0.027	0.589	0.67	0.142	0.07	0.044	0.015	12.81	2.83	8.45	0.31	14.65	4.63
Spring C52	12/07/04	6.482	5.56	34.6	0.091	0.018	0.018	0.068	0.046	0.051	0.054	0.066	0.48	0.157	0.02	0.01	0.00	71.89	2.84	10.03	2.24	20.33	6.06
C52	28/09/04	6.535	5.88	34.4	0.094	0.018	0.019	0.07	0.048	0.052	0.058	0.664	0.42	0.155	0.06	0.01	0.00	76.00	3.00	10.14	2.20	21.72	6.23
C52	13/12/04	6.446	6.44	31.9	0.091	0.018	0.019	0.069	0.047	0.053	0.055	0.664	0.42	0.155	0.06	0.01	0.00	76.00	3.00	10.14	2.20	21.72	6.23
C52	03/05/05	6.250	6.23	28.8	0.078	0.016	0.017	0.067	0.037	0.05	0.05	0.6	0.74	0.128	<0.01	0.00	0.05	72.40	2.99	10.00	1.13	18.44	5.64
C52	31/05/05	6.117	6.30	30.2	0.082	0.017	0.017	0.07	0.04	0.05	0.065	0.661	0.57	0.131	<0.01	0.00	0.16	72.40	2.41	12.42	0.05	19.29	6.01
C52	11/02/06	6.246	6.27	29.7	0.087	0.017	0.017	0.069	0.047	0.053	0.055	0.664	0.57	0.131	<0.01	0.00	0.16	72.40	2.41	12.42	0.05	19.29	6.01
C52	22/08/05	6.450	6.47	29.5	0.093	0.017	0.017	0.069	0.047	0.053	0.055	0.664	0.57	0.131	<0.01	0.00	0.16	72.40	2.41	12.42	0.05	19.29	6.01
C52	07/02/06	6.678	6.24	32.3	0.092	0.019	0.018	0.069	0.047	0.055	0.057	0.664	0.57	0.131	<0.01	0.00	0.16	72.40	2.41	12.42	0.05	19.29	6.01
C52	03/04/06	6.756	6.04	31.2	0.073	0.018	0.018	0.073	0.031	0.049	0.067	0.664	0.88	0.107	0.06	0.01	0.00	59.98	2.45	10.60	0.18	19.65	5.81
C52	10/02/06	6.389	6.05	32.5	0.087	0.017	0.017	0.067	0.047	0.053	0.055	0.664	0.57	0.131	<0.01	0.00	0.16	72.40	2.41	12.42	0.05	19.29	6.01
C52	21/08/06	6.298	6.3	33.1	0.084	0.017	0.018	0.068	0.039	0.056	0.063	0.588	0.58	0.151	0.02	0.00	0.00	70.57	2.54	10.76	0.30	19.65	5.84
C52	02/10/06	6.300	6.3	32.3	0.082	0.023	0.018	0.072	0.05	0.048	0.065	0.557	0.59	0.129	0.05	0.01	0.00	75.40	2.78	11.63	0.32	20.41	6.19
C52	Average	6.015	6.015	28.5	0.076	0.016	0.016	0.064	0.045	0.051</													

887

888 Table 1: Chemical compositions of spring and stream waters, open field precipitation, throughfalls
889 under spruces (PL5) and beeches (PLH). The total dissolved solids (TDS_w) have been calculated
890 from the major dissolved elements concentrations (cations, anions and silica) and are expressed in
891 mg/L. as calculated for several watersheds (e.g.. Gaillardet et al., 1999). Another parameter, called
892 here $TDS-Ca$ ($=Ca+Mg+Na+K+SiO_2+Fe$) has been calculated as proposed by Zakharova et al.
893 (2007) and reflects the silicate weathering.

894

895

Samples	date	⁸⁷ Sr/ ⁸⁶ Sr	2sigma	²³⁴ U/ ²³⁸ U	2sigma	altitude (m)
Spring CS1	28/09/04	0.72573	0.00002	0.880	0.001	1080
CS1	13/12/04	0.72656	0.00004	0.875	0.005	1080
CS1	29/03/05	0.72780	0.00001	0.892	0.003	1080
CS1	22/05/06	0.72650	0.00001	0.886	0.002	1080
CS1	Average	0.72665		0.883		
Spring CS2	03/05/05	0.72546	0.00001			1055
CS2	11/07/05	0.72376	0.00001			1055
CS2	22/05/06	0.72544	0.00001	0.875		1055
CS2	02/10/06	0.72515	0.00001			1055
CS2	Average	0.72495		0.875		
Spring CS3	13/12/04	0.72325	0.00002	0.823	0.003	1098
CS3	29/03/05	0.72328	0.00001	0.827	0.003	1098
CS3	11/07/05	0.72314	0.00002			1098
CS3	22/05/06	0.72325	0.00001	0.819	0.004	1098
CS3	Average	0.72323		0.823		
Spring CS4	03/05/05	0.72490	0.00002	0.866	0.003	1050
CS4	11/07/05	0.72375	0.00001			1050
CS4	22/05/06	0.72353	0.00001	0.867	0.002	1050
CS4	02/10/06	0.72548	0.00001			1050
CS4	Average	0.72442		0.867		
Spring BH	12/07/04	0.72262	0.00002	1.106	0.005	915
BH	13/12/04	0.72289	0.00002	1.1	0.003	915
BH	29/03/05	0.72359	0.00001	1.101	0.003	915
BH	03/05/05	0.72340	0.00001	1.1	0.003	915
BH	31/05/05	0.72319	0.00001	1.112	0.003	915
BH	11/07/05	0.72279	0.00001	1.101	0.003	915
BH	22/08/05	0.72287	0.00001	1.106	0.003	915
BH	03/10/05	0.72307	0.00001	1.105	0.003	915
BH	22/05/06	0.72334	0.00002	1.099	0.004	915
BH	Average	0.723084		1.103		
Spring RUZS	13/12/04	0.72700	0.00002	0.945	0.004	950
RUZS	29/03/05	0.72665	0.00001	0.941	0.003	950
RUZS	22/05/06	0.72669	0.00001	0.949	0.003	950
RUZS	Average	0.72678		0.945		
Spring RH	28/09/04	0.72206	0.00008	0.996	0.003	980
RH	13/12/04	0.72240	0.00002	0.991	0.004	980
RH	29/03/05	0.72257	0.00002	0.993	0.005	980
RH	22/05/06	0.72242	0.00001	0.991	0.004	980
RH	Average	0.72236		0.993		
Spring SG	28/09/04	0.72353	0.00002	0.91	0.004	1093
SG	13/12/04	0.72328	0.00007	0.93	0.003	1093
SG	29/03/05	0.72352	0.00002	0.923	0.004	1093
SG	22/05/06	0.72354	0.00002	0.927	0.002	1093
SG	Average	0.72347		0.923		
Spring SH	28/09/04	0.72749	0.00003	0.916	0.003	1050
SH	13/12/04	0.72720	0.00009	0.915	0.003	1050
SH	29/03/05	0.72801	0.00002	0.914	0.004	1050
SH	03/05/05	0.72798	0.00001			1050
SH	22/05/06	0.72720	0.00001	0.911	0.004	1050
SH	02/10/06	0.72752	0.00001			1050
SH	Average	0.72757		0.914		
Outlet RS	29/03/05	0.72573	0.00002	0.939	0.003	883
RS	22/05/06	0.72520	0.00001	0.974	0.004	883
RS	Average	0.72547		0.957		
atmospheric inputs	Average					
Rain	2004-2006	0.7111		1.175		
Throughfalls spruces	2004-2006	0.71290		1.079		
Throughfalls beeches	2004-2006	0.71620		0.953		
clays SS under beeches	35 cm depth	0.872847	0.00002	1.26	0.003	
clays SS under beeches	95 cm depth	0.767439	0.00001	1.074	0.002	
clays NS under spruces	35 cm depth	0.830034	0.00001	1.094	0.002	
clays NS under spruces	95 cm depth	0.802886	0.00001	nd		

896

897 Table 2: Sr isotopic compositions and U AR for spring waters, outlet, rain, throughfalls and clays
898 (Prunier, 2008) from the Strengbach watershed. Clays SS: clays from a soil profile located on the
899 southern slope and under beeches, and clays NS: clays from a soil profile located on the northern
900 slope and under spruces.

901

2004-2006	water fluxes (mm)	Na fluxes mg/m2/yr	K fluxes mg/m2/yr	Mg fluxes mg/m2/yr	Ca fluxes mg/m2/yr	Si fluxes mg/m2/yr	Sr fluxes µg/m2/yr	U fluxes µg/m2/yr
rain - F_{rain}	1247	306	219	56	256	5	1.1	7.6
throughfall - $F_{throughfall}$	1070	1041	3037	256	1034	101	2.4	12.6
<i>biological contribution to throughfalls C_b (1.2.3.4)</i>		0.2	0.9	0.3	0.25	0.1	nd	nd
Atmospheric contribution to throughfall - $F_{throughfall(corrected)}$		833	304	179	776	91	nd	nd
global atmospheric input (a)	1096	754	291	161	697	78	1.1 to 2.4	7.6 to 12.6
outlet fluxes (b)	850	1634	608	456	2276	3008	8.8	113
rain-corrected outlet fluxes (c)	850	1328	388	399	2019	3003	7.7	105
(wet+dry atmos. deposits)-corrected outlet fluxes (d)	850	880	317	295	1579	2929	7.7 to 6.6	105 to 101

902

903 Table 3: Elementary fluxes for rain, throughfalls and outlet in the Strengbach catchment. The rain
 904 corresponds to open field precipitations, the throughfalls have been collected under spruces (80% of
 905 the forest cover) and beeches (20% of the forest cover). The chemical composition of throughfalls
 906 includes wet and dry atmospheric deposition and biological excretion (biological leaching). In order
 907 to estimate the atmosphere-derived fluxes (input fluxes) we applied for every element a specific
 908 corrective factor C_b (1) Ulrich et al. 1983; (2) Dambrine et al., 1998; (3) Thimonier et al., 2008. (4)
 909 Berger et al., 2008. The global atmospheric input has been calculated considering the catchment
 910 area as 15% of clearing and 85% of forest, the formula is then: $F_{atm} = 0.15 F_{rain} + 0.85 F_{throughfall(corrected)}$.

911 The outlet fluxes correspond to the catchment export fluxes (b).

912

913

914

915

916

917

918

919

Soils under spruces - Northern slope (1)																									
depth	SiO2	Al2O3	MgO	CaO	Fe2O3	MnO	TiO2	Na2O	K2O	P2O5	Mg/Ca	Mg/Na	Ca/Na	muscovite	Quartz	K-Feld	plagio	apatite	Smectite	amorph	smectite (%)	OM	pH	Clays	CEC
cm	%	%	%	%	%	%	%	%	%	%	%	%	%	%	%	%	%	%	%	%	in clay fract.	%		%<2µm	cmol/kg
10	72.74	17.84	0.51	0.06	1.92	0.04	0.24	0.62	5.70	0.22	7.56	1.34	0.18	42.2	38.6	10.9	5.4	0.05	3.7	0.68	19.7	7.5	3.7	22.2	15.49
50	64.82	20.71	0.66	0.15	2.43	0.04	0.32	0.85	5.60	0.43	3.65	1.27	0.35	50.1	27.3	5.6	0.21	5.8	1.09	19.8	9.2	4.4	20.3	11.98	
70	65.89	20.59	0.65	0.28	2.12	0.03	0.22	0.99	5.59	0.52	1.95	1.07	0.55	47.5	27.8	7	8.7	0.42	6	1.11		7	4.4	15.8	10.37
90	66.10	20.44	0.70	0.28	2.04	0.02	0.20	0.92	5.71	0.43	2.10	1.24	0.59	45.4	27.4	8.9	8.1	0.43	7.8	0.89		6.3	4.5	12.5	9.78
110	67.17	19.82	0.61	0.30	2.40	0.03	0.20	1.22	5.90	0.47	1.71	0.81	0.47	40.2	27.2	12.8	10.6	0.43	6.4	0.9	27.1	5.1	4.6	8.1	9.79
130	65.25	21.10	0.58	0.39	1.84	0.02	0.22	1.87	5.81	0.49	1.26	0.50	0.40	42.5	22.1	10.7	16.4	0.54	5.1	0.87		5.7	4.7	6.9	9.23
150	65.68	21.82	0.59	0.32	1.86	0.02	0.20	2.04	5.63	0.42	1.52	0.47	0.31	46.5	21.9	7.2	17.8	0.42	4.3	0.7		5.3	4.7	5.1	8.68
170	69.31	20.18	0.60	0.31	1.60	0.03	0.17	1.81	5.77	0.35	1.64	0.54	0.33	39.4	26.9	12.6	15.9	0.41	6.4	0.54		3.8	4.7	4.2	9.76
190	67.17	19.22	0.70	0.28	1.79	0.01	0.27	1.35	5.81	0.32	2.10	0.85	0.40	34.2	25.9	15.5	11.6	0.39	10.2	0.46		6.2	4.6	5.3	15.19
210	68.03	19.51	0.64	0.31	1.42	0.01	0.24	1.37	6.23	0.33	1.73	0.75	0.44	34	25.9	17.9	11.8	0.44	8.5	0.41	47.8	5.6	4.6	5.2	13.94

Soils under beeches - Southern slope (1)																									
depth	SiO2	Al2O3	MgO	CaO	Fe2O3	MnO	TiO2	Na2O	K2O	P2O5	Mg/Ca	Mg/Na	Ca/Na	muscovite	Quartz	K-Feld	plagio	apatite	Smectite	amorph	smectite (%)	OM	pH	Clays	CEC
cm	%	%	%	%	%	%	%	%	%	%	%	%	%	%	%	%	%	%	%	%	in clay fract.	%		%<2µm	cmol/kg
4	74.45	14.21	0.33	0.18	1.21	0.01	0.33	1.90	4.77	0.25	1.54	0.28	0.18	18.9	39.5	18.9	14.7	0.15	4.4	0.54	14.7	12	4.0	13.3	7.86
15	72.52	15.87	0.34	0.13	1.27	0.01	0.31	1.85	5.41	0.22	2.23	0.30	0.13	23.9	36.5	20	13.6	0.1	3.8	0.41		6.7	4.1	11.6	7.7
35	69.10	15.96	0.35	0.10	2.16	0.04	0.29	1.70	4.96	0.60	2.99	0.34	0.11	23.1	35.1	17.8	12.5	0.05	4.3	2.14		12.3	4.6	10.7	8.00
52.5	66.96	17.53	0.40	0.13	2.52	0.05	0.31	1.81	4.98	0.45	2.65	0.36	0.14	26.3	31.7	15.9	13.4	0.1	5	2.7	22.2	11.9	4.8	8.7	5.02
77.5	65.03	18.61	0.47	0.16	2.85	0.06	0.30	1.91	4.96	0.57	2.46	0.40	0.16	28.7	28.6	14.4	14.3	0.15	6.1	2.89		10.9	4.8	6.3	4.24
100	66.10	18.82	0.55	0.22	2.39	0.08	0.36	1.67	5.24	0.40	2.14	0.53	0.25	31	29.5	14.7	11.8	0.27	7.6	1.63	27.7	7.7	4.8	4.2	4.08
122.5	65.25	19.48	0.56	0.26	1.96	0.08	0.29	1.83	5.34	0.42	1.83	0.50	0.27	33.4	27.3	13.9	13.1	0.33	7.4	1.22		7.5	4.8	3.1	3.6
150	63.54	20.46	0.55	0.32	2.72	0.11	0.28	2.22	5.52	0.45	1.45	0.40	0.28	33.8	22.7	14.8	16.6	0.4	7.1	1.43		6	4.9	2.5	2.6
177.5	64.82	19.35	0.48	0.26	2.85	0.10	0.24	2.47	5.48	0.41	1.56	0.32	0.20	28.1	23.3	17.9	19.1	0.28	6.5	1.17		5.2	4.9	1.8	2.12
177.5	65.89	18.31	0.45	0.29	2.83	0.10	0.28	2.44	5.36	0.44	1.30	0.30	0.23	24	25.3	19.5	19	0.33	6.5	1.19		5.1	4.9	1.6	1.79
200	62.25	20.22	0.55	0.33	3.73	0.15	0.33	2.59	5.04	0.52	1.39	0.34	0.25	31.9	20.9	12.7	20.2	0.39	7.4	1.48	19.8	6.2	4.9	2.1	1.79

Soils - Gneiss (2)																		
depth	SiO2	Al2O3	MgO	CaO	Fe2O3	MnO	TiO2	Na2O	K2O	P2O5	Mg/Ca	Mg/Na	Ca/Na	muscovite	Quartz	K-Feld	plagio	apatite
cm	%	%	%	%	%	%	%	%	%	%	%	%	%	%	%	%	%	%
30	62.84	15.25	1.00	0.20	5.72	0.15	0.77	0.42	3.44	0.43	4.22	3.87	0.92	nd	nd	nd	nd	nd
65	69.61	15.20	1.35	0.13	5.27	0.09	0.71	0.38	3.93	0.24	8.77	5.77	0.66	nd	nd	nd	nd	nd
135	68.00	15.41	1.22	0.09	5.99	0.09	0.70	0.25	4.23	0.23	11.44	7.93	0.69	nd	nd	nd	nd	nd
175	71.88	15.61	1.02	0.24	3.11	0.04	0.56	0.05	4.71	0.23	3.59	33.16	9.24	nd	nd	nd	nd	nd
225	64.97	16.11	0.86	0.12	9.26	0.16	0.59	0.10	4.69	0.19	6.05	13.98	2.31	nd	nd	nd	nd	nd

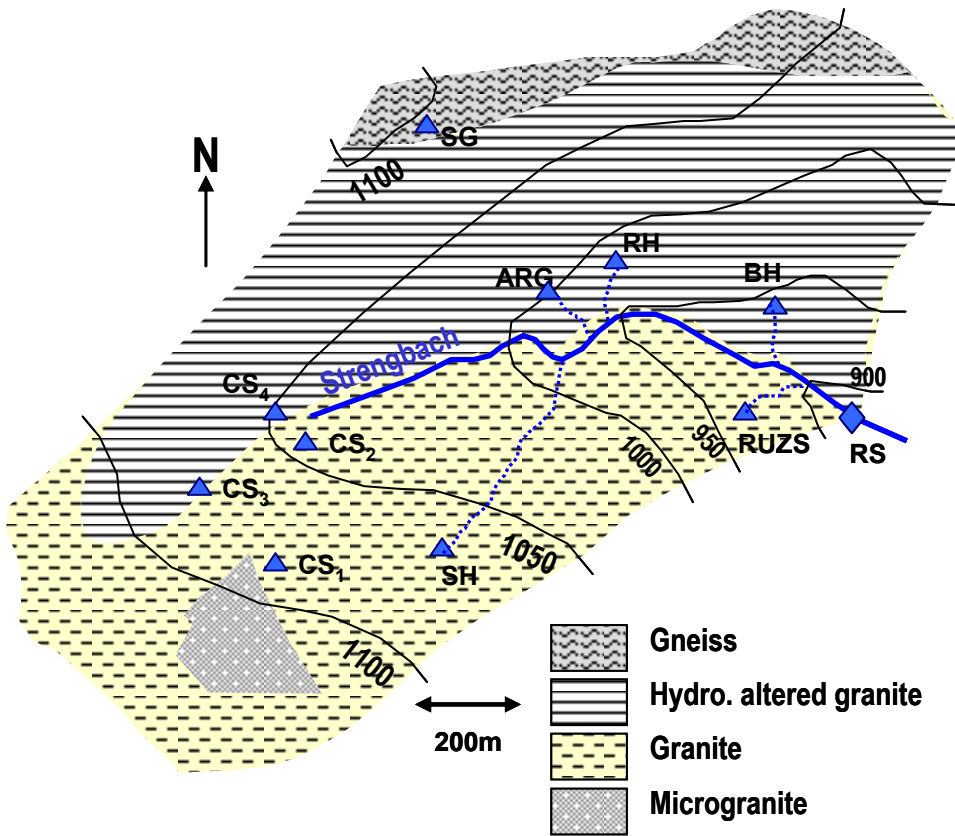
Bedrock - average value (1), (2), this study																		
cm	SiO2	Al2O3	MgO	CaO	Fe2O3	MnO	TiO2	Na2O	K2O	P2O5	Mg/Ca	Mg/Na	Ca/Na	muscovite	Quartz	K-Feld	plagio	apatite
%	%	%	%	%	%	%	%	%	%	%	%	%	%	%	%	%	%	%
Northern slope	75.38	14.50	0.45	0.29	1.38	0.03	0.19	0.98	6.19	0.31	1.31	0.75	0.57	29	49	19	2	0.5
Southern slope	74.13	14.32	0.26	0.36	0.98	0.01	0.18	2.87	5.70	0.33	0.61	0.15	0.24	13	34	30	22	0.5
Gneiss	65.08	17.95	2.55	0.20	7.59	0.07	0.89	0.55	4.13	0.12	10.63	7.54	0.71	nd	nd	nd	nd	nd

920
921

922 Table 4: Chemical and mineralogical compositions of soils and bedrocks from the Strengbach

923 watershed. (1): Fichter, 1997, (2): El Gh'Mari, 1995.

924
925



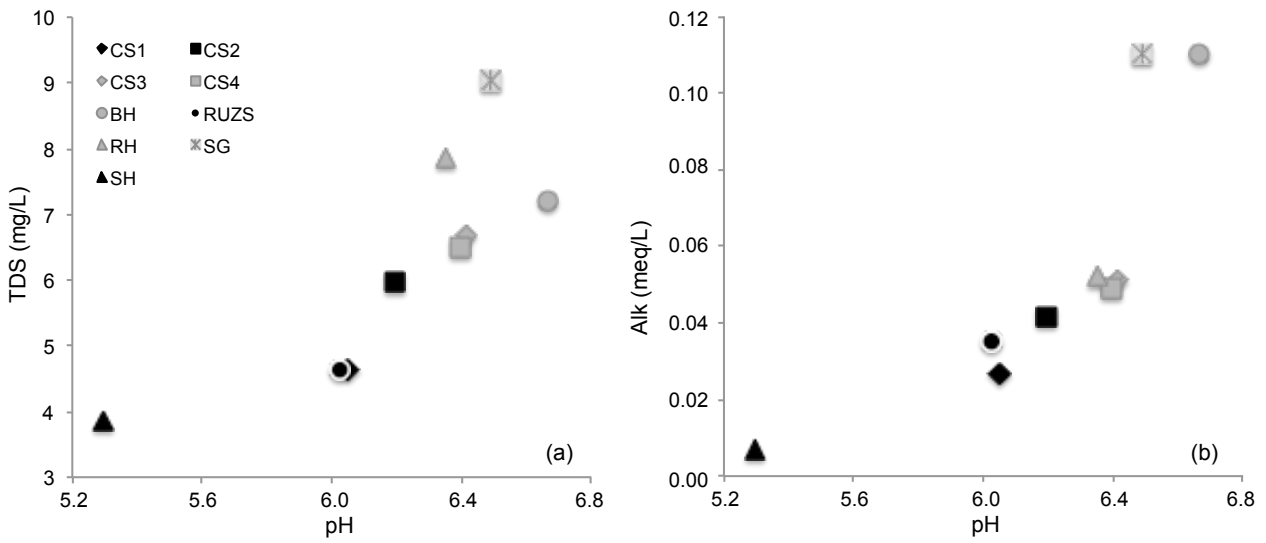
927

928 Fig. 1: Map of the Strengbach catchment showing the principal lithological units and the location of
 929 the 10 studied springs (SG, RH, ARG, BH, CS₁, CS₂, CS₃, CS₄, SH, RUZS). RS corresponds to
 930 the Strengbach stream at the outlet of the studied catchment.

931

932

933

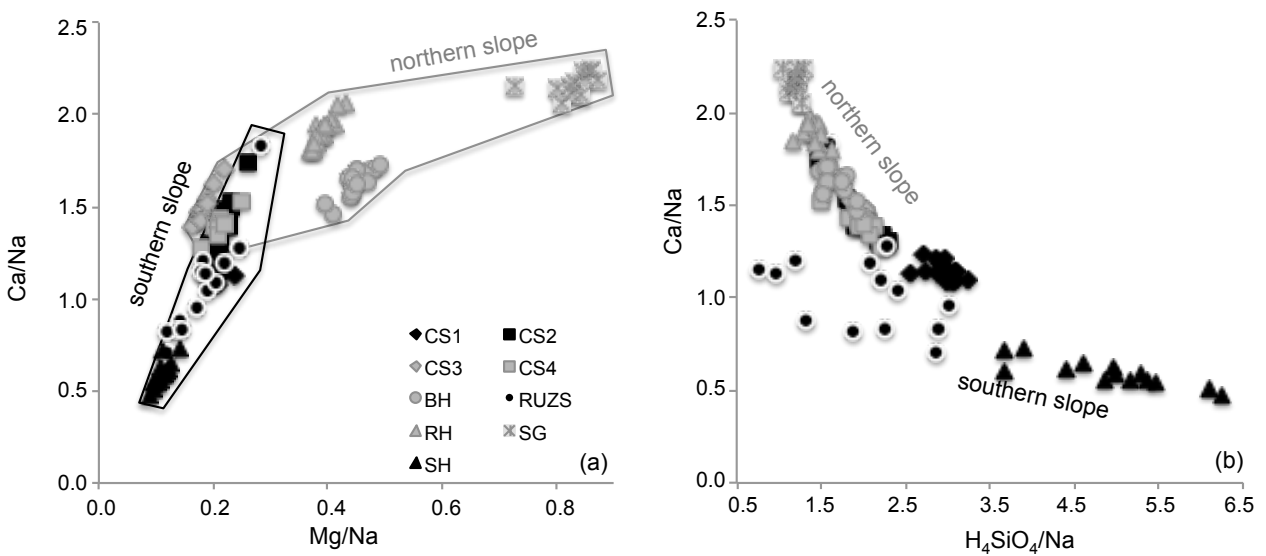


934

935 Fig. 2: Physico-chemical characteristics of the different source waters of the Strengbach watershed
936 (average values for the period 2004-2006). a) pH vs TDSw and b) pH vs Alk.

937

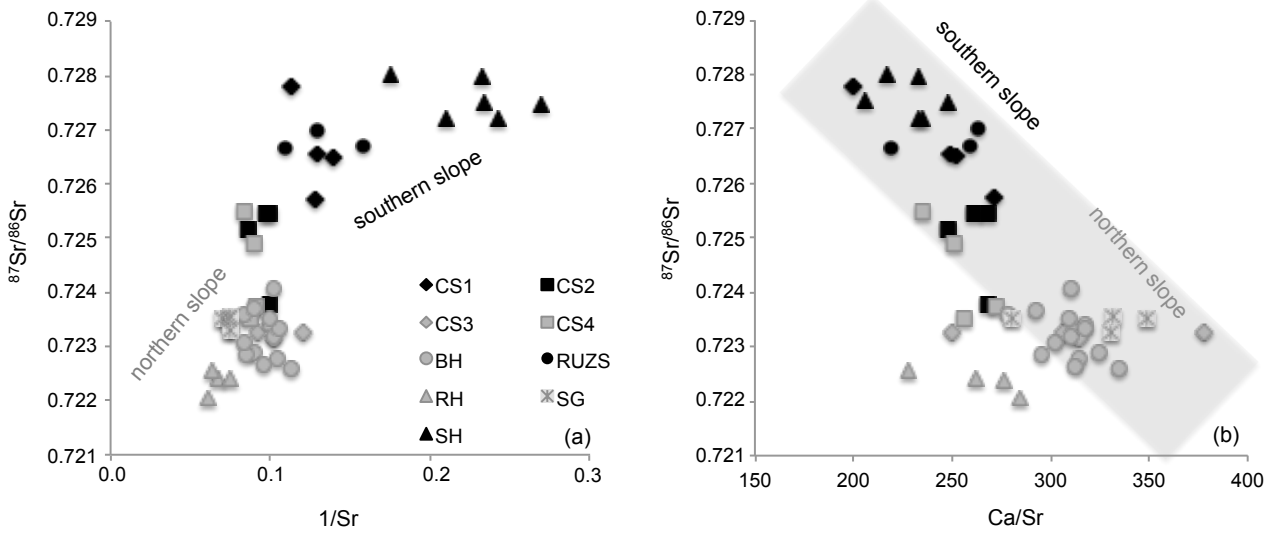
938



939

940 Fig. 3: Major element concentration ratios of the 9 different individual source waters of the
941 Strengbach watershed. a) Ca/Na vs Mg/Na and b) Ca/Na vs Si(OH)₄/Ca. In each diagram the spring
942 waters from the southern slope show different compositions than those from the northern slope.

943

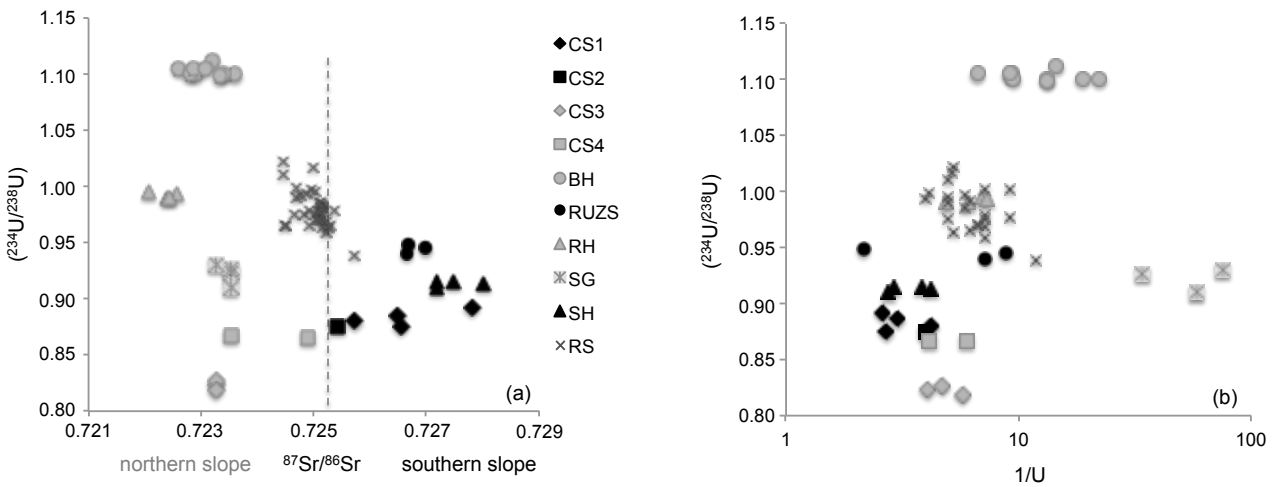


944

945 Fig. 4: Relationships between $^{87}\text{Sr}/^{86}\text{Sr}$ isotope ratios and a) $1/\text{Sr}$ (ppb); b) Ca/Sr (ppb/ppb). The
 946 isotope ratios allow a clear distinction between northern and southern slope sources.

947

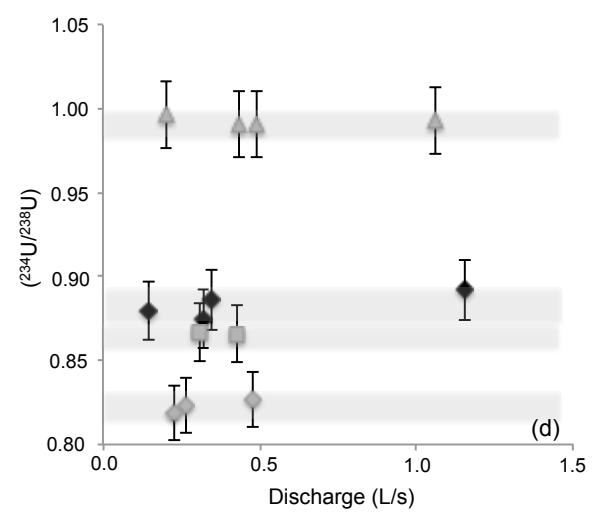
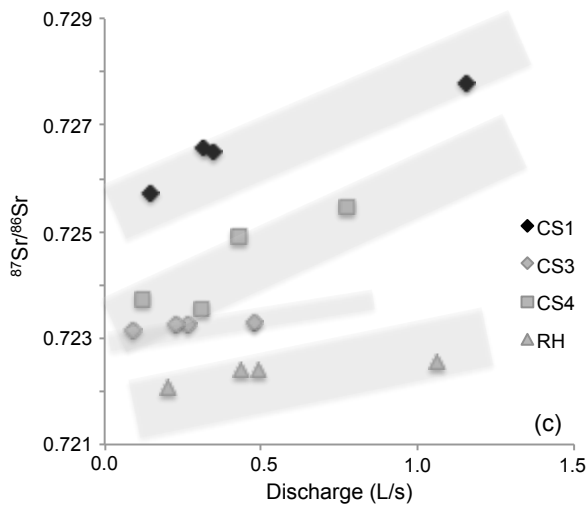
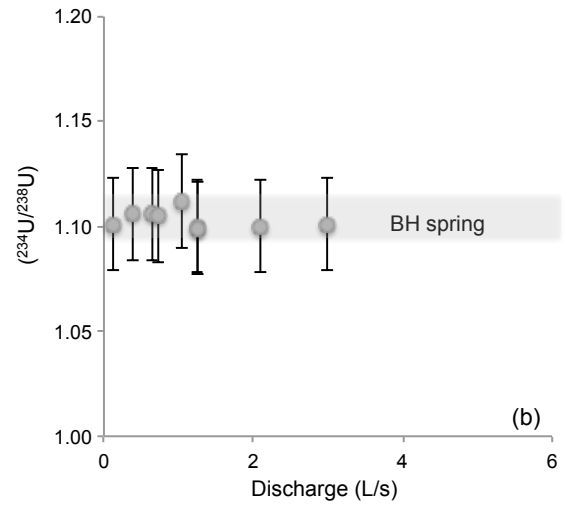
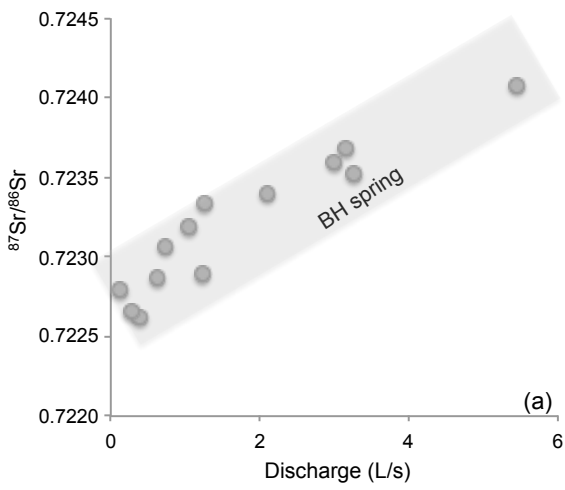
948



949

950 Fig. 5: Relationship between $(^{234}\text{U}/^{238}\text{U})$ AR and a) $1/\text{U}$ and, b) $^{87}\text{Sr}/^{86}\text{Sr}$. In contrast to Sr isotopic
 951 compositions, the U AR of springs do not allow to distinguish between the northern and southern
 952 slopes.

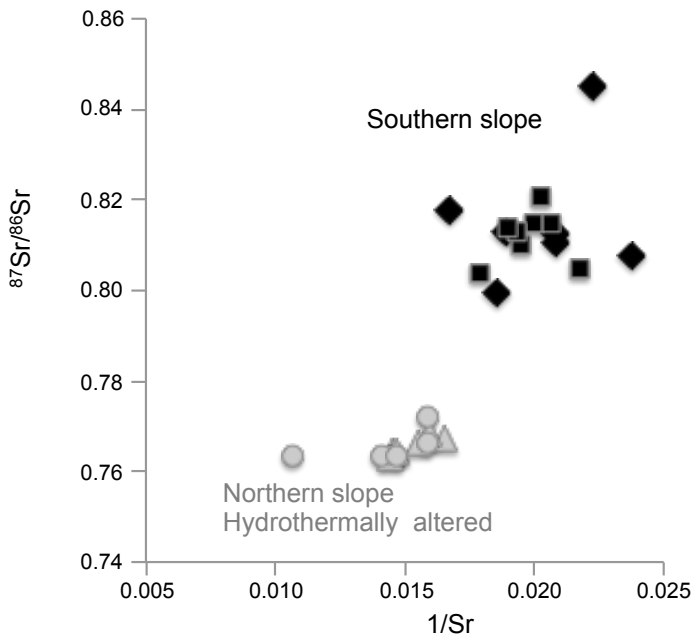
953



954

955 Fig. 6: $^{87}\text{Sr}/^{86}\text{Sr}$ and $(^{234}\text{U}/^{238}\text{U})$ AR vs discharge for the springs BH, CS1, CS3, CS4 and RH from
 956 the Strengbach watershed.

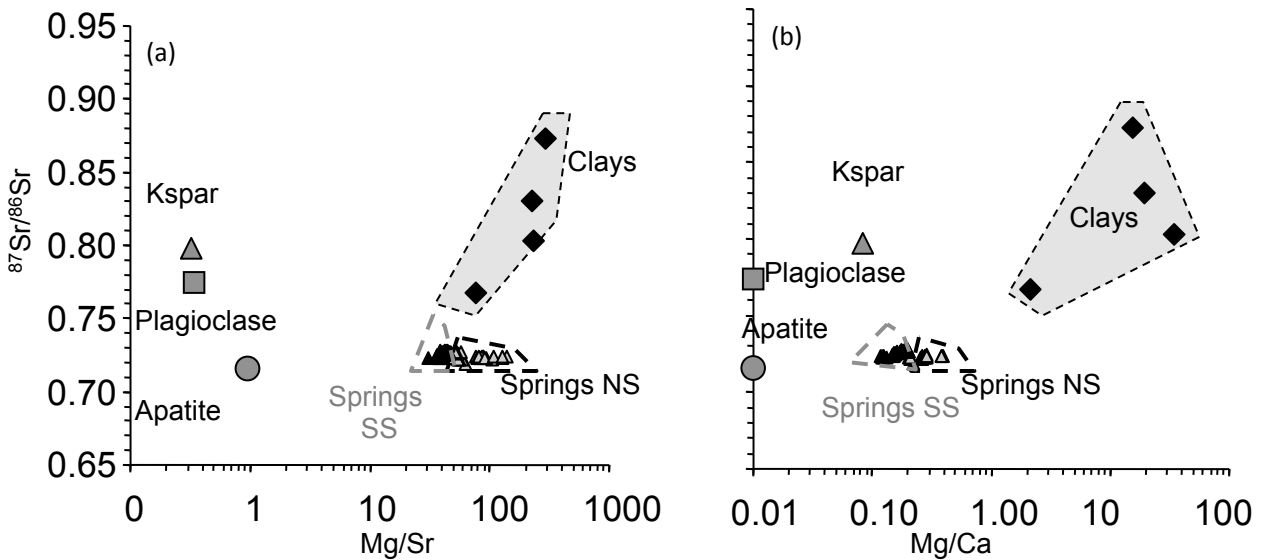
957



959

960 Fig. 7: $^{87}\text{Sr}/^{86}\text{Sr}$ vs $1/\text{Sr}$ for the soil and saprolite samples from the Strengbach watershed. The
 961 samples from the northern slope and those from the southern slope are clearly different (Aubert,
 962 2001; Stille et al., 2009 ; Prunier, 2008).

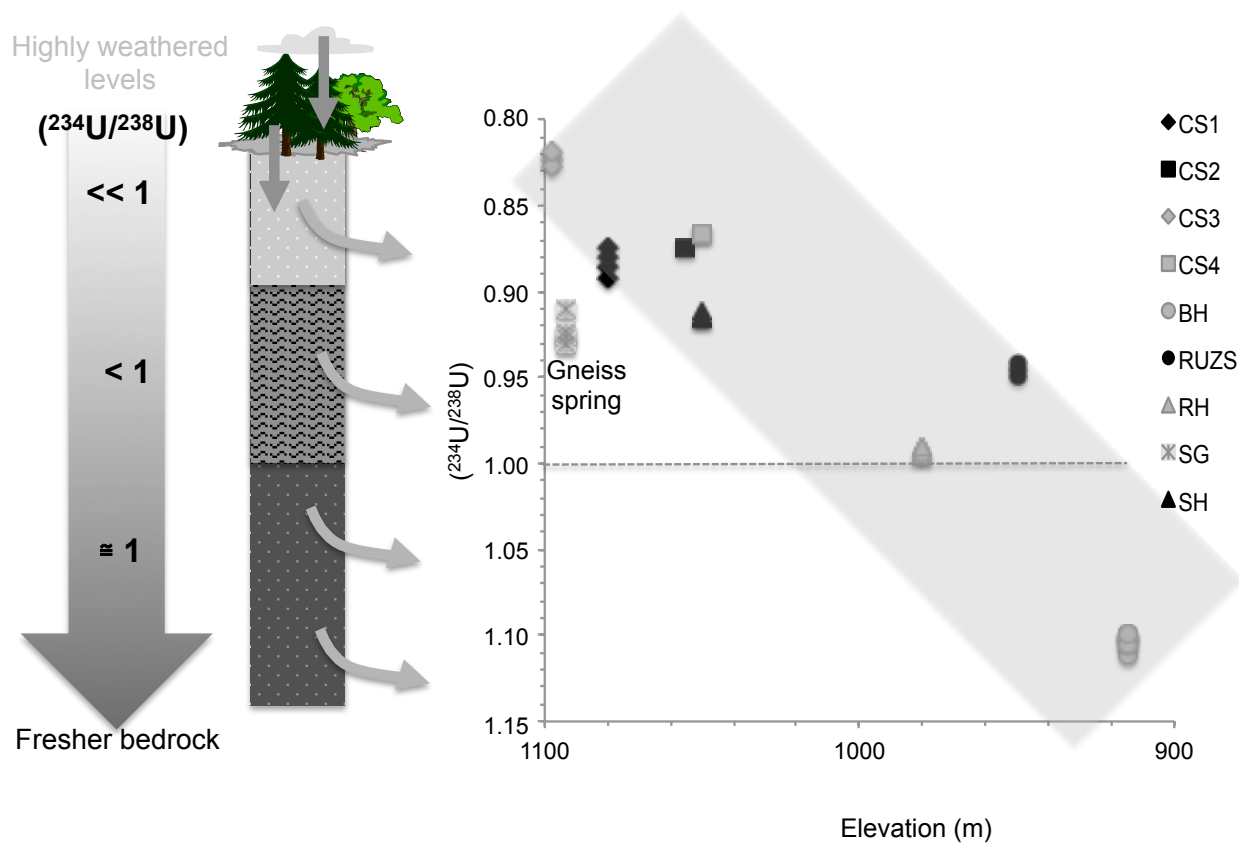
963



964

965 Fig. 8: $^{87}\text{Sr}/^{86}\text{Sr}$ vs Mg/Ca (a) and Mg/Si (b) for the spring waters (NS = northern slope and
 966 SS=southern slope), primary minerals of the granite (Aubert et al.. 2001) and clays from soils
 967 (Prunier, 2008).

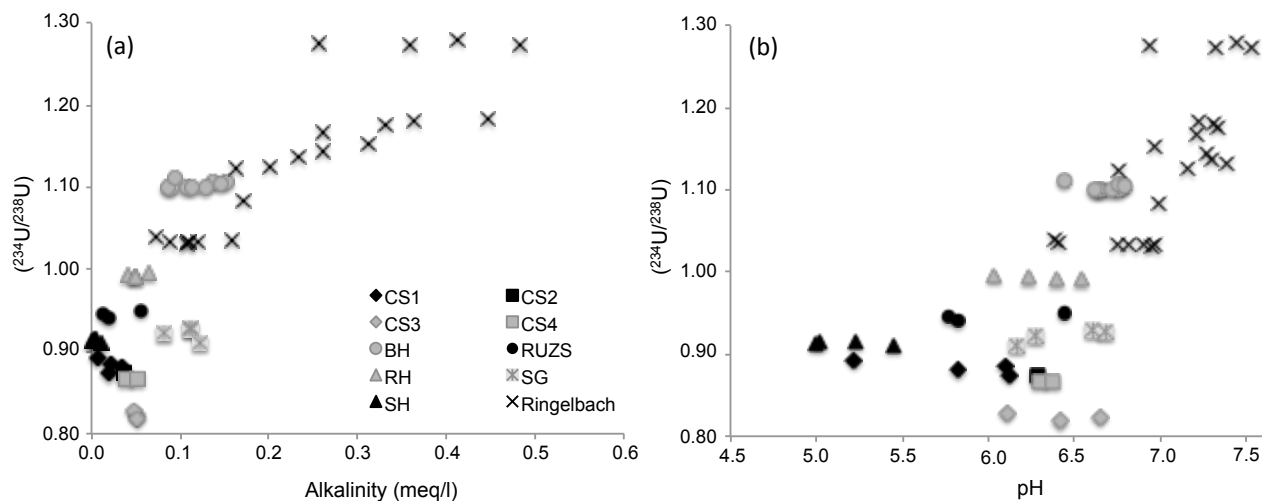
968



969

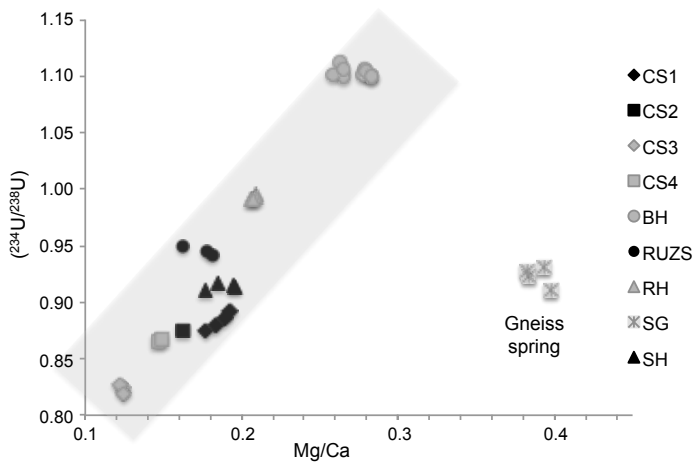
970 Fig. 9: $(^{234}\text{U}/^{238}\text{U})$ AR of springs vs elevation. The U AR increase with decreasing altitude at the
 971 catchment scale.

972



973

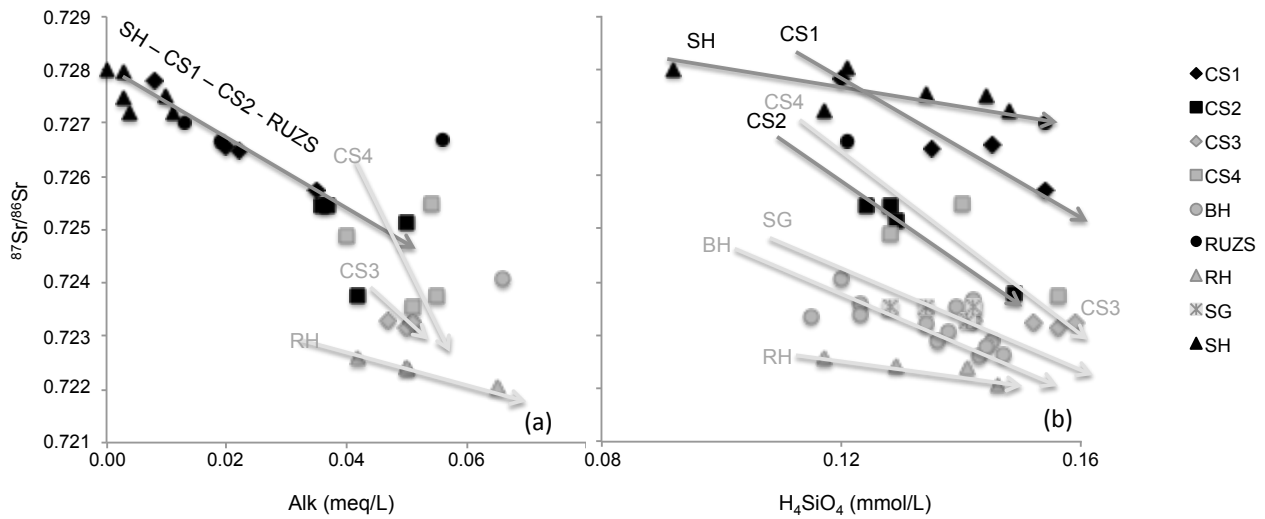
974 Fig.10: Variations of $(^{234}\text{U}/^{238}\text{U})$ AR vs a) alkalinity and b) pH in the springs from the Strengbach
 975 and Ringelbach (Shaffauser et al., 2014) watersheds.



976

977 Fig. 11: Variations of $(^{234}\text{U}/^{238}\text{U})$ AR vs Mg/Ca ratio in the springs. The U AR are positively
 978 correlated with the Mg/Ca ratios.

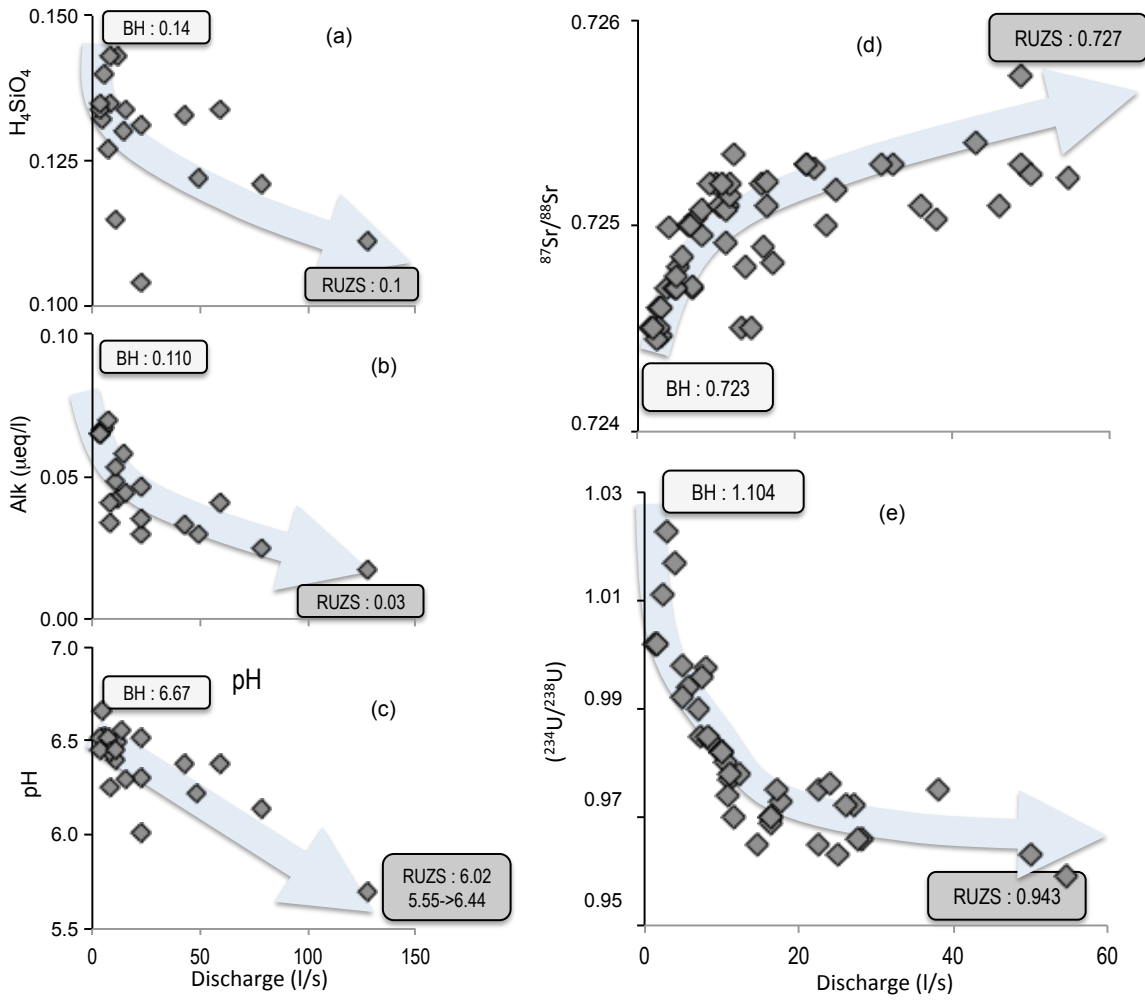
979



980

981 Fig. 12: $^{87}\text{Sr}/^{86}\text{Sr}$ vs alkalinity (a) and Si concentrations (b) for the springs from the Strengbach
 982 watershed. For each of the individual spring the $^{87}\text{Sr}/^{86}\text{Sr}$ ratios decrease with increasing alkalinity
 983 and Si content.

984



985

986 Fig. 13: H_4SiO_4 concentration (a), alkalinity (b), pH (c), $(^{234}U/^{238}U)$ AR (d) and $^{87}Sr/^{86}Sr$ (e) vs
 987 discharge at the outlet for the 2004-2006 period (additional data from Riotte et al. (1999) and
 988 Aubert et al., (2002)).

989

990

991

992